Suspension Bridges. The Aerodynamic Problem and Its Solution

Les problèmes aérodynamiques du pont suspendu et leurs solutions

Die aerodynamischen Probleme und ihre Lösungen bei Hängebrücken

D. B. Steinman, Consulting Engineer, New York, N. Y.

This is the story of a baffling scientific problem with which the engineering profession was dramatically confronted in 1940, and of the ensuing intensive application of the resources of science and invention for the urgent solution of the problem.

On July 1, 1940 the Tacoma Narrows Bridge at Puget Sound was completed and opened to traffic. Built at a cost of $ 6,400,000, with a main span of 2800 feet, it was the third longest span in the world. On November 7, 1940, four months and six days after the official opening, the oscillations of the bridge in a mild gale (fig. 1) increased to destructive amplitude until the main span broke up, ripping loose from the cables and crashing into the water 208 feet below (fig. 2) [1, 2].

The engineering fraternity was startled by the catastrophe. The phenomenon was not new, but had been unrecorded or forgotten by the profession. A century earlier, bridge after bridge had been similarly wrecked by wind action, notably the Brighton Chain Pier in England in 1836, the Wheeling Bridge over the Ohio River in 1854, the Lewiston-Queenston Bridge over Niagara River in 1864, and the Niagara-Clifton Bridge at Niagara Falls in 1889 [4]. John A. Roebling (1806—1869) taught the profession the importance of adequate stiffening of suspension bridges; his bridges stood up while those built by his contemporaries were wrecked by the wind. But a later generation of engineers, forgetting the lesson of the past, began to preach the virtues of flexibility without recalling its hazards. This reversal of trend reached its climax in the ill-fated Tacoma span [1, 2].
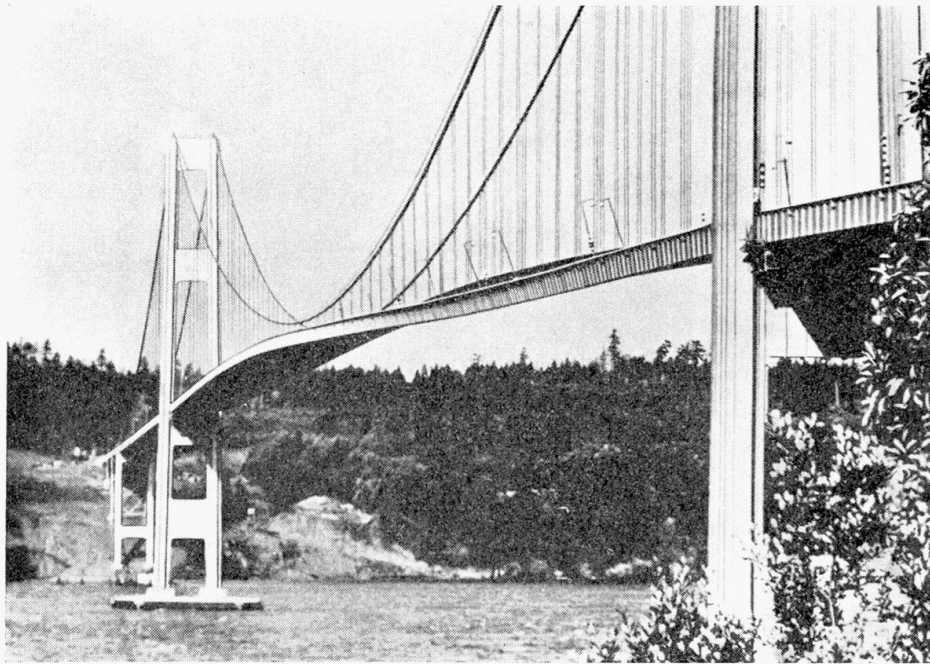
Fig. 1. Catastrophic Aerodynamic Oscillations of the Tacoma Narrows Bridge. Torsional Oscillations, November 7, 1940. Maximum Double Amplitude, 28 feet.

Fig. 2. Aerodynamic Destruction of the Tacoma Narrows Bridge. November 7, 1940.

In fact, some twenty known bridges completed since 1930 have been subject to disturbing or dangerous aerodynamic oscillations, and some of them have required the application of corrective measures to make them safe. In 1945, a contract of over $1,300,000 was let for additional stiffening and correction of the 2300-foot-span Bronx-Whitestone Bridge [10]. The Golden Gate Bridge, with the world's longest span of 4200 feet, has suffered dangerous aerodynamic oscillations and in 1953 a contract for over $3,000,000 was let for stiffening the structure against aerodynamic action.

The decade ending in 1940 witnessed more rapid progress in bridgebuilding, as measured by lengthening spans, boldness of proportions, and increasing magnitude of projects, than all the centuries preceding. The five longest spans in the world were all completed during this decade, and the record span length was more than doubled, from 1850 feet to 4200 feet. The startling problem to which the profession was awakened in 1940 threatened to halt further progress in long-span bridges.

Recognizing that a complete, scientific solution of this challenging problem was desperately needed, I dedicated myself to the task. In fact, I discovered the aerodynamic action in 1938 and promptly commenced my intensive studies, two years before the Tacoma Bridge failure [1, 2]. I have devoted fifteen years of my professional life (1938 to 1953) to the solution of this problem. It has required the creation of a new science, combining the essentials of three different fields of specialized knowledge — the deflection theory of suspension bridges, the science of aerodynamics, and the mathematical theory of vibration analysis. Even existing knowledge in aerodynamic science proved inadequate, necessitating new research, new invention, and creative mathematical analysis [12, 13].

Aerodynamic Instability

The *aerodynamic* action of wind is something new in the thinking and science of bridge engineers. Their prior thinking (since the failure of the Tay Bridge in Scotland in 1879) had been limited to the *aerostatic* action of wind [3].

On July 29, 1944, another bridge disaster occurred. A two-span continuous truss bridge (fig. 3) over the Mississippi River at Chester, Illinois, was blown off its piers by the wind [3].

The failure of the Tacoma Narrows Bridge dramatically exemplified the aerodynamic effect of wind, while the Chester Bridge failure exemplified the aerostatic effect. The two are related; and both disasters had their lessons for the profession.

Since the Tay Bridge disaster in 1879, bridges have been designed for the horizontal pressure of wind. But bridge specifications and textbooks made no mention of wind *uplift*. Aeronautic engineers, of course, knew the significance of the vertical component, or *lift*. But the bridge engineer continued to work in a separate, insulated compartment of technical knowledge [3 ,9].

Fig. 3. Continuous Truss Bridge over the Mississippi River at Chester, Illinois. Destroyed by Wind, July 29, 1944.

The Tacoma Bridge failure should have directed the attention of bridge engineers to the significance of the vertical component of horizontal wind pressure. In 1941 (in a published discussion [8] a year before the Chester Bridge was built), I called attention to the fact that wind uplift on a bridge may amount to three or four times the horizontal pressure, but that fact was overlooked by the designers of the Chester Bridge [3, 9].

The *aerostatic* problem, as exemplified by the Chester Bridge failure, is comparatively simple and elementary. The *aerodynamic* problem, as exemplified by the Tacoma Bridge failure and by the alarming oscillations of other suspension bridges, is one of much greater difficulty and complexity.

The Tacoma Bridge was adequately safe for all of the loads and forces for which it had been designed, namely dead load, live load, temperature, and the *static* effect of wind load. It had not been designed ,however, for the *aerodynamic* effect of wind load [1, 2].

By *aerodynamic instability* we mean: *the effect of a steady wind, acting on a flexible structure of conventional cross-section, to produce a fluctuating resultant force automatically synchronizing in timing and direction with the harmonic motions of the structure so as to cause a progressive amplification of those motions to dangerous or destructive amplitudes* [4].

On the morning of the Tacoma Bridge failure, the gale of 35 to 42 miles an hour meant a horizontal wind pressure of little more than *five* pounds per square foot of vertical surface. The bridge had been designed for a horizontal wind pressure of *fifty* pounds per square foot and was structurally safe for a static wind load of that magnitude. It was destroyed, however, by the *cumulative* dynamic effect of the *vertical* components produced by a horizontal wind pressure of only five pounds per square foot [1, 2].

Thus the Tacoma span was the victim of its extreme flexibility and of the vulnerability of its cross-section to the creation of resultant wind forces producing *cumulative amplification of oscillations*. This combination constitutes *aerodynamic instability* [4].

Related Phenomena of Instability

The problems of aerodynamic and hydrodynamic stability include such instability phenomena as the "singing" of telephone wires; the "galloping" of electric transmission lines; the transverse vibrations of submarine periscopes, of towing cables, and of other submerged parts of naval equipment; the lateral vibrations of tall smoke stacks; the wind-induced vertical oscillations of suspended pipe lines; the flutter of airplane wings and control surfaces; and the wind-induced oscillations of flexible bridge spans. All of these phenomena are related in that they all involve vibrations initiated or amplified by drawing energy from the relative flow of the surrounding fluid medium.

These stability problems are challenging to the engineer because the attendant vibrations may have serious effects, including impairment of usefulness (as in periscopes), increase in drag (as in airplane parts), fatigue failure (as in telephone wires), rupture from abnormal stress (as in transmission lines), and physical destruction (as in the catastrophic oscillations of a bridge) [10].

The instability problem of bridge oscillations has probably been the most complex and the most challenging. Its comprehensive solution has contributed to the solution of some of the related instability problems.

In the classification and differentiation of these vibration problems, two categories of instability phenomena need to be distinguished: *forced vibrations*, and *self-excited vibrations* [10, 11].

In a *forced vibration*, the alternating force that initiates, amplifies and sustains the vibration exists independently of the vibration and persists even when the vibratory motion is stopped. Moreover, the frequency of the alternating force is independent of the natural frequency of the vibration, and amplification depends upon *accidental* resonance or proximity to resonance. Hydrodynamic vibrations of cylinders (vibrations identified with vortex shedding) belong in this category.

In a *self-excited vibration*, the alternating force that amplifies and sustains the oscillation is created or controlled by the oscillation itself. In this case, the alternating force is *automatically* resonant with the natural (or forced) frequency of the oscillations. In such automatic resonance, the relative phase or direction of the alternating force created by the vibration determines aerodynamic *stability* or *instability*. The galloping of ice-coated transmission lines, the flutter of airplane surfaces, and the oscillations of flexible bridge spans belong in this classification [5, 10, 11, 12].

Hydrodynamic Oscillations of a Cylinder

When a cylinder moves transversely at a uniform velocity through a fluid, or when a fluid moves steadily past a stationary immersed cylinder, eddies are shed periodically from the cylinder, forming the KÁRMÁN vortex trail. Each time an eddy is released, an unbalanced lateral force acts on the cylinder. If the cylinder is free to vibrate laterally, the alternating lateral forces may impose on it a forced vibration with a frequency equal to the eddy frequency. If the eddy frequency f is in a critical range related to the natural frequency N of the cylinder, the vibration of the cylinder may attain a high amplitude [10].

The eddy frequency f depends only on the diameter d of the cylinder and on the relative stream velocity V, by the simple relation

$$f = S \frac{V}{d} \tag{1}$$

where S is a dimensionless ratio, first determined by V. STROUHAL in 1878. For Reynolds numbers between 500 and 200,000, the Strouhal number S may be taken as practically constant at $S \approx 0.20$. This dimensionless ratio fd/V or $V/(fd)$, or the corresponding expression for other cases, is the basic parameter in the formulation of all vibration phenomena related to the velocity of fluid flow. (In self-excited oscillations, as in bridges, the corresponding parameter is Nb/V or $V/(Nb)$, where N is the natural frequency of the structure and b is the width of the cross-section.)

The circulation Γ of an eddy in the vortex trail is given by

$$\Gamma \approx 1.71 \; Vd \tag{2}$$

The circulation about the cylinder at any instant is the algebraic sum of the circulations of all the vortices in the wake. When the steady state of V is reached the circulation about the cylinder is not $\pm \Gamma$, but $\pm \frac{1}{2}\Gamma$. (This point has been missed in prior literature on the subject.) The resulting alternating lateral force L acting on the cylinder is [10].

$$L \approx 1.71 \; (\tfrac{1}{2}\rho \, V^2)\, d \tag{3}$$

This transverse lateral force L is nearly twice as large as the direct horizontal drag D. As alternate eddies are shed and trail off in the double-row wake, L is a periodically alternating force, with frequency f, acting on the cylinder. This force L acts downward when the eddy is shed from the top of the circular section, and upward when the eddy leaves the bottom of the circular section. This periodically alternating force L is capable of initiating oscillations from a state of rest, also of amplifying them until a steady state of oscillation is reached.

A common misconception needs correction. The oscillations of the cylinder (or other section) are not caused or produced *by the vortices*. The vortices in the

wake are merely counters, markers, or footprints providing a convenient physical and mathematical trail from which the circulation about the cylinder and the consequent lateral forces acting on the cylinder may be inferred, formulated, and computed [10, 13].

Recent test results indicate significant modified relations when the immersed cylinder is actually oscillating: If the cylinder is in transverse vibration due to the action of its vortex trail, it sheds an eddy at or near each end of its ampli-
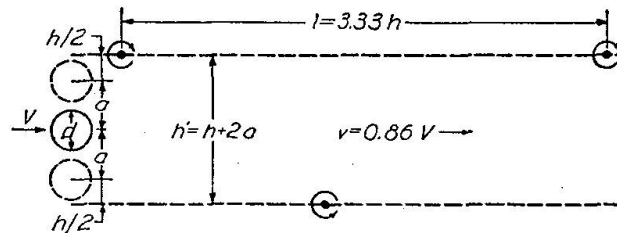

Fig. 4. Vortex Trail in Wake of Oscillating Cylinder.

tude range (fig. 4). Consequently the normal width (h) of the vortex street is augmented by the total amplitude $(2\,a)$, or in the ratio.

$$q = (h + 2\,a)/h \tag{4}$$

The stability geometry of the vortex trail requires the wave length between eddies to be increased in the same ratio. Hence the drag D, the circulation Γ, and the lateral force L are all increased in the same ratio q; and the Strouhal number S and the eddy frequency f are reduced in the inverse ratio [10].

Upon substituting for L and f their changing values in terms of the values L_0 and f_0 at zero amplitude, my derived equation for oscillation amplitudes becomes:

$$a = \pm\, \frac{q\,(L_0/K)}{1 - \left(\frac{1}{q}\,\frac{f_0}{N}\right)^2} \tag{5}$$

where K is the "spring constant" (the force of restitution per unit displacement). Eq. (5) is here given in simplified form, with the damping term omitted. In eq. (5), q is a function of the unknown amplitude a. For convenience of numerical or graphical solution, eq. (5) is resolved into a pair of simultaneous equations. My graphic solution, applied to a typical example, yields the results plotted in fig. 5. In fig. 5, BF and DD are the stable steady states, and EE is the unstable steady state. The problem of predicting the stability or instability, and the amplitudes, of a cylinder (such as a periscope) vibrating in a relative stream flow at varying velocities V had previously defied mathematical solution. Fig. 5 checks and explains the test results previously obtained in hydraulic laboratories. It also explains an observed anomaly that had always puzzled naval experts, namely the fact that, at certain speeds (in the instability range),
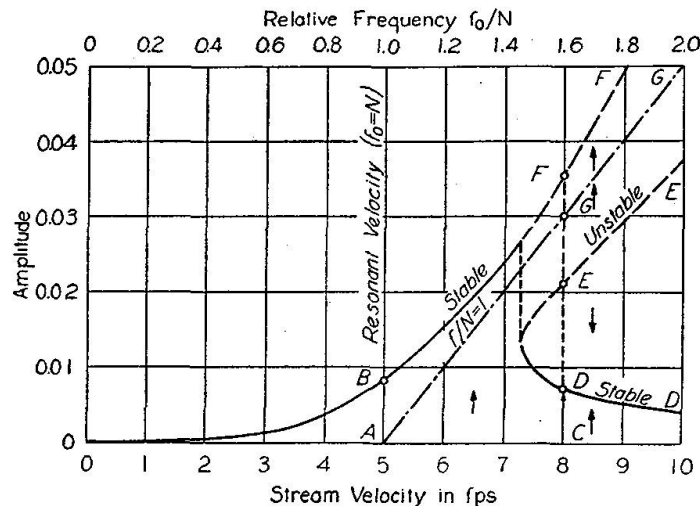
Fig. 5. Amplitude — Response Graph for Oscillating Cylinder by Vortex Theory. —
(Author's Solution of the Periscope Problem.)

a periscope is sometimes violently oscillating (as at F in fig. 5) and, at the same speeds on other occasions, it is virtually free of vibration (as at D in fig. 5). [10]

In 1951, I was retained to stabilize a pipeline bridge of 700-foot span over the Coosa River in Alabama. Dangerous vertical oscillations at low wind velocities threatened to destroy the suspended pipeline through fatigue failure; such an accident would have been catastrophic from the standpoint of the natural-gas-pipeline transmission company. The contractors had applied various damping and restraining devices, including suspended sea-anchors and dynamic (spring-type) vibration absorbers, but vertical oscillations of serious amplitude persisted [11].

My solution was to install a light system of diagonal wire-rope stays (fig. 6) so as to form trussing between each main cable and the suspended pipeline. This economical solution proved highly successful, virtually eliminating the aerodynamic oscillations. The amplitudes were reduced from the prior observed values as high as three feet to the present maximum of a fraction of an inch (with the dynamic vibration absorbers and emergency sea-anchors discarded) [11].

Included in my studies on this engagement were tests of various methods of modifying the exposed sections of the cylinders so as to break up the aerodynamic circulation (Γ), represented by the KÁRMÁN vortex trail, and thus remove the cause of the instability of the span. Several shapes of vanes and fairing were tested on my office models and in the wind-tunnel of the Virginia Polytechnic Institute. In this case, however, the estimates of cost indicated that such installations would cost two or three times as much as the simple cable-stay system adopted [11].

The aerodynamic instability of a cylinder must be distinguished from the aerodynamic instability of conventional bridge cross-sections. The two are
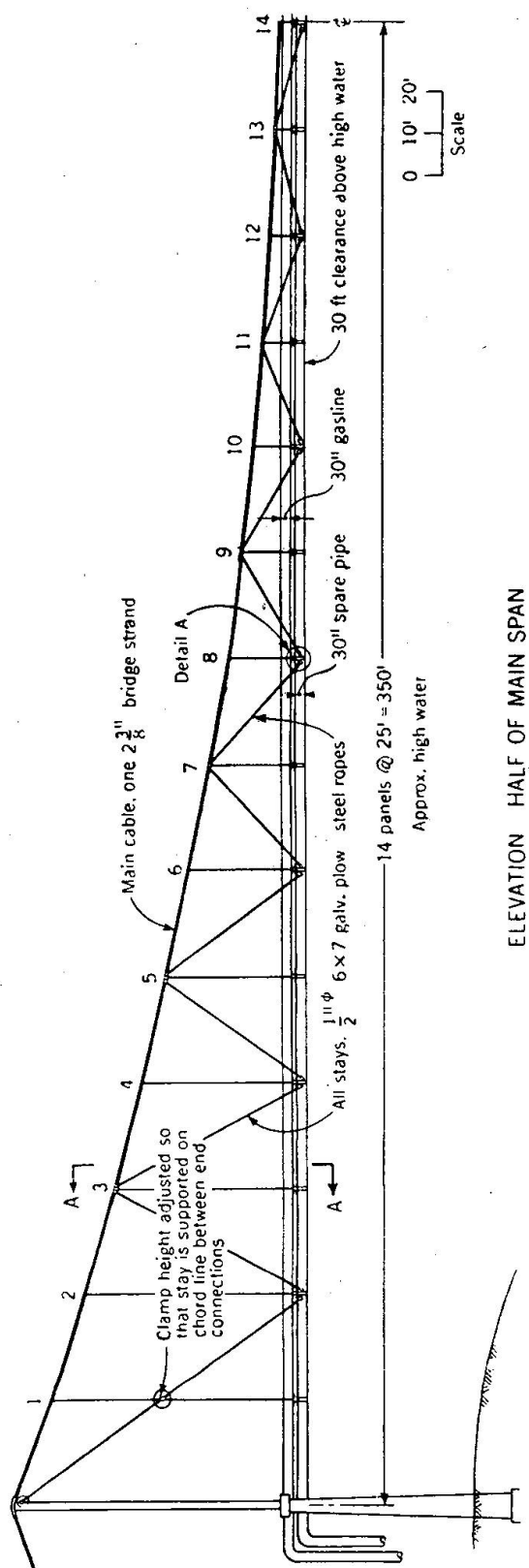
Fig. 6. Pipeline Bridge Stabilized with Diagonal Rope Stays. (Coosa River, Alabama, 1951.)

contrasting phenomena, although the manifestations and catastrophic conse-
quences may be similar. Different test criteria apply and the mathematical
analysis is quite different. The instability problem for the conventional sus-
pension bridge is more difficult, and the mathematical solution is far more
complex.

Some attempts have been made to explain the aerodynamic oscillations of
suspension bridges in terms of "vortex-shedding" or "vortex-buffeting", but
such investigations or speculations have not yielded any useful contributions
toward the scientific and practical solution of the problem [12].

Self-Excited Oscillations

The self-excited oscillations of shapes or sections of relatively narrow width
are first considered. This is the problem typified by "the galloping" of ice-
coated transmission lines.

Certain shapes or sections, when exposed to a steady wind (or other steady
fluid flow), will build up rapidly amplifying oscillations which, oddly enough,
are transverse to the wind. Such shapes or sections are called *unstable*. Examples
(fig. 7) are a half-round with flat face toward the wind, a T-section with head
toward the wind, a flat vertical plate, a deep H-section, a deep U-section,
etc. [5, 10].

When upward inclined wind (R, fig. 7) strikes the flat vertical face of such
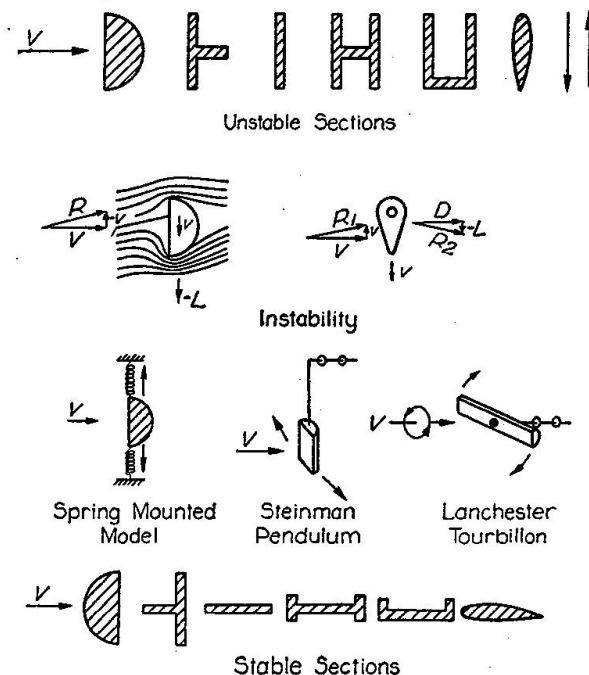section, the stagnation point is above mid-height. This point determines the

Fig. 7. Aerodynamically Stable and Unstable Sections. Explanation, Identification, and
Elementary Demonstrations.

division of the airflow, and hence the greater part of the flow has to pass around the lower edge of the section. This crowding of the flow lines represents increased flow velocity and, consequently (by Bernoulli's Theorem), a reduction of pressure. Accordingly, we have the paradox: *Upward* inclined wind (R_1, fig. 7) produces a *downward* inclined resultant (R_2, fig. 7). This paradox is always identified with aerodynamically *unstable* sections [10].

In the case of these elementary sections, *downward* motion of the section compounded with horizontal flow of the fluid produces a *relatively upward* angle of incidence (R, R_1, fig. 7). This, in turn, produces a *downward* resultant pressure (R_2, fig. 7). Hence an *unstable* section is subjected to a downward resultant wind action whenever the section is moving down and an upward resultant wind action whenever the section is moving up; consequently the oscillation is *amplified*. The amplifying force of the wind is thus created and controlled *by the oscillation*, so that it is automatically synchronous with the oscillation, always in the same direction as the oscillation, and always in perfect phase with the oscillation *velocity* [5, 10].

Ice coating on transmission lines tends to form a vertically elongated section which belongs to the unstable category (R_1, R_2, fig. 7). This explains the violent oscillations or "galloping" of such lines in high wind, with potential amplitudes of destructive magnitude. Vertical motions of 20 feet have been recorded. Various damping devices have been developed to reduce or prevent such oscillations. The high amplitudes help to show that these oscillations (self-excited) and those of cylindrical sections (vortex action) are quite different phenomena; the latter have amplitudes limited to approximately 1.5 diameters.

For the self-excited oscillations (fig. 7), the oscillation frequency is the natural frequency of the oscillating system, and is independent of the wind velocity. Any increase in wind velocity increases the amplification. At high wind velocity, the oscillation may become catastrophic [10].

It is important to note that these self-excited oscillations are always *transverse* to the direction of the fluid flow. Oscillations in the direction of the flow are damped (by the air flow).

An effective demonstration (fig. 7) is provided by mounting the section model between light springs. When the steady wind from a fan or blower is applied head-on, the slightest vibration, even an imperceptible tremor, is rapidly amplified (at a logarithmic rate) to a violent oscillation of maximum amplitude.

The "Steinman pendulum" (fig. 7) affords another striking demonstration. The section model is mounted vertically on a rigid pendulum rod suspended from an axis parallel to the wind. The oscillations, initiated seemingly from a state of rest, are soon built up to pendulum swings of startling magnitude.

A still more instructive demonstration is the "Lanchester tourbillon" (fig. 7). If the section model of an *unstable* section is pivoted at the center and mounted as a pitchless propeller, exposure to the head-on breeze of an electric

fan will develop a rapidly *accelerated* spin in a direction *opposite* to the spin of the fan.

The distinguishing feature of unstable sections, as illustrated by the paradox of the Lanchester pinwheel, is the *reversed* direction of the resultant. An upward inclined fluid flow against the stationary section will produce a *downward* resultant. Any section having this hydrodynamic characteristic is an unstable section [5, 10].

On the other hand, certain other shapes or sections, when similarly mounted with spring or pendulum to permit transverse oscillation, will not be set into amplified oscillation by exposure to a steady wind or other steady fluid flow. Any imposed initial oscillation will be aerodynamically damped. Such shapes are aerodynamically *stable* sections. Examples (fig. 7) are a half-round with convex side toward the wind, a *T*-section with stem toward the wind, a horizontal flat plate, a shallow *H*-section, a shallow *U*-section, or any streamlined or airfoil section. Any of these sections, when mounted as a pitchless propeller and exposed to the head-on breeze of an electric fan, will develop a normal uniform spin in the *same* direction as the spin of the span. If the wind is without spin, the pitchless propeller of *stable* section will not be self-starting, and any rotation artificially imparted to the propeller will be brought to rest by the wind. The distinguishing feature of *stable* sections is that an upward inclined fluid flow against the stationary section will produce an *upward* resultant [5, 10].

Wind-Tunnel Tests

A convenient scientific method of determining the aerodynamic characteristics of a section, including its classification and behavior as a stable or unstable section, is by means of wind-tunnel tests. In a *static* wind-tunnel test, the section model is held stationary, at successive angles of incidence. The aerodynamic reactions are lift, drag, and moment of lift. By plotting the dimensionless coefficients C_D, C_L, and C_M, against angle of incidence (α), one obtains the static drag, lift, and moment (or torque) graphs, respectively (fig. 8) [10].

The ordinates C_D, C_L, and C_M of the respective graphs are defined by the three fundamental equations of aerodynamics: [12]

$$D = C_C \left(\tfrac{1}{2}\rho\, V^2 b\right) \tag{6 a}$$

$$L = C_L \left(\tfrac{1}{2}\rho\, V^2 b\right) \tag{6 b}$$

$$M = C_M \left(\tfrac{1}{2}\rho\, V^2 b^2\right) \tag{6 c}$$

The *"slopes"* (or angular gradients) of the static lift and torque graphs (after correction for drag) are significant. They are defined by [12, 13].

$$s_1 = \frac{\partial C_L}{\partial \alpha} \tag{7 a}$$

$$s_2 = \frac{\partial C_M}{\partial \alpha} \tag{7 b}$$

DRAG GRAPH

STABLE LIFT GRAPH

UNSTABLE LIFT GRAPH
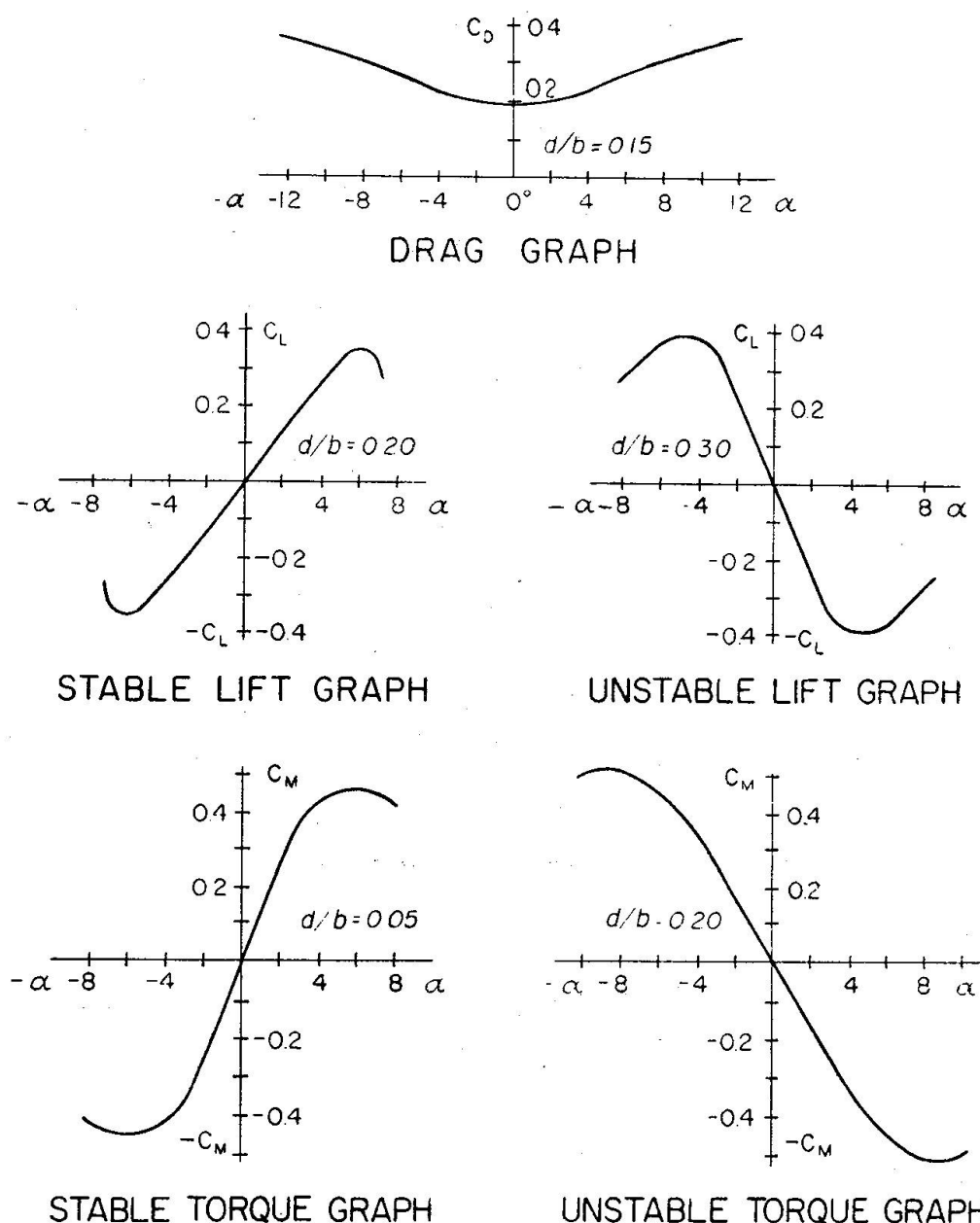
STABLE TORQUE GRAPH

UNSTABLE TORQUE GRAPH

Fig. 8. Drag, Lift, and Torque Graphs for H-sections. Identification of Stable and Unstable Sections.

The slope of the static *lift* graph determines the *vertical* stability or instability of the section (fig. 8). A static lift graph with a central range of *positive* slope identifies an aerodynamically *stable* section. The steeper this positive slope, the greater will be the vertical stability of the section. A static lift graph with a central range of negative slope identifies an aerodynamically unstable section. The steeper the *negative* slope, the greater will be the vertical instability of the section [10, 12].

Similar relations of the static *moment* graph (supplemented by the corresponding graphs for a *curved* model, a new concept introduced by me) determine the *angular* stability or instability of wider sections [13].

Aerodynamic Instability of Narrow Sections

The relative increase per cycle in the amplitude (*a*), or the *logarithmic increment* per cycle, is denoted by δ:

$$\delta = \frac{\Delta a}{a} = \frac{\Delta W}{2W} \tag{8}$$

where *W* is the total energy in the oscillating system. The logarithmic increment or rate of amplification δ is the measure of *instability*. The logarithmic increment δ, applied to any initial amplitude, is like a rate of compound interest, compounded at each oscillation [12].

For pure *vertical* oscillations of a narrow section (or of a wide section at very high wind velocities *V*), the logarithmic increment or rate of amplification is given by:

$$\delta_1 = -\tfrac{1}{4} \cdot \frac{\rho b^2}{m} \cdot s_1 \cdot \frac{V}{NB} \tag{9}$$

where *N* is the frequency of the oscillations, *b* is the width of the section, *m* is the mass per linear foot of span, and ρ is the air density in mass per unit volume. Each factor in eq. (9) is dimensionless [12].

The dimensionless factor $\rho b^2/m$ is the "density-mass ratio". Upon substituting standard values of ρ and *g*, this factor reduces to $0.0766\, b^2/w$ in units of feet and pounds [12].

The dimensionless factor $V/(Nb)$ is the "reduced velocity" or the "velocity ratio". It is the controlling parameter in all aerodynamic studies [5, 12].

The minus sign in eq. (9) corresponds to the *identification of unstable* sections. If the slope s_1 is negative, the logarithmic increment δ_1 is positive, denoting *amplification*.

Aerodynamic Instability of Wide Sections

This is the problem of the aerodynamic instability of flexible bridge spans, flexible towers, and other structures [5, 10].

The problem is properly and logically separable into two parts:

1. *The Solid Mechanics Problem:* To determine (predictively) the normal modes and natural frequencies of potential oscillations, and the amplification producible by any given energy input.

2. *The Fluid Mechanics Problem:* To determine the net energy transfer from a given steady fluid flow to a specified oscillating boundary surface, and to devise forms of boundary profile that will minimize or reverse the energy transfer.

The elastic or *solid mechanics* phase of the problem is comparatively easy. All parts of it are readily answered by known fundamental relations of suspension bridge analysis and vibration mechanics, and the final equations for

practical application can be expressed in very simple, convenient formulas. Simple integration yields formulas that will answer all questions on oscillation modes and frequencies more accurately and expeditiously than the most elaborate and spectacular large-scale model tests. Unfortunately much valuable time and effort have been misdirected by investigators to this elementary part of the problem, in costly experimentation and in voluminous and needlessly formidable mathematical analysis, to the neglect of the more basically important and more difficult part of the study — the *aerodynamic* problem [10].

The aerodynamic or *fluid mechanics* phase of the problem has been challenging. It has involved not only new and illuminating applications of known concepts, but also the extension of the field to the exploration and establishment of new relations and new concepts. To say that the problem was too complicated for scientific formulation and predictively valid solution was not helpful. The problem was critical and had to be solved. I outlined and finally developed, on a scientific foundation, a comprehensive solution that explains the phenomena and permits predictive design and control. My complete solution yields coefficients of rigidity, natural oscillation periods and modes, velocity relations, energy relations, critical wind velocities, rates of amplification, limiting amplitudes, design criteria and specifications, and methods of predicting, testing, checking, and preventing aerodynamic instability [12, 13].

Effect of Phase Difference

In comparison with the elementary sections previously discussed, the new feature introduced with the wider sections is the *time* required for the fluid flow, or for any disturbance in the fluid flow, to traverse the width of the section. This introduces a new factor — *phase difference*. A flow disturbance, initiated at the leading edge, takes *time* to traverse the width and encounters a progressively increasing difference of phase as it traverses the oscillating section. As different points of the width are reached, different stages of the cycle of oscillation are encountered, including differences of velocity and even differences of direction of motion [10, 12].

Strange as it may seem, this seemingly obvious basic concept was missed by other investigators. Without it, the problem could not be solved.

The elementary expression for energy input per cycle is

$$\Delta W = \pi.P.a.\cos\phi \qquad (10)$$

where a is the amplitude, P is the harmonic amplifying force, and ϕ is the phase difference between amplifying force and *velocity* of displacement. The multiplier $\cos\phi$ is the correction factor in multiplying two vectors differing by the angle ϕ in direction or phase (illustrated by the "power factor" applied to the product of volts by amperes in alternating current) [10, 12, 13].

In the wider sections here under consideration, if the horizontal fluid flow is at *high velocity* so as to make the phase difference across the width of the section relatively negligible, the same governing relations will obtain as in the elementary sections of narrow width. An *unstable* section (s_1 negative) will be subjected to a downward resultant whenever it is moving down and an upward resultant whenever it is moving up. Amplifying force will be in phase with velocity of displacement, yielding a maximum value for energy input ($\phi = 0$ in eq. 10). This high velocity range in which the phase difference becomes negligible has no upper limit and is therefore called the *catastrophic range*. In the same high velocity range (ϕ negligible) a *stable* section (s_1 positive) will be subjected to an upward resultant whenever it is moving down and a downward resultant whenever it is moving up. The energy input will be negative (P negative or $\phi = \pi$, in eq. 10), so that any oscillation will be damped [10, 12].

Hence there is one vitally important difference between stable and unstable sections, namely: *A basically unstable section (s negative) will have an upper critical range that is unlimited, and therefore potentially catastrophic.*

Both categories of sections, however, have lower critical ranges of minor potential instability (fig. 9). Since ϕ varies across the width of the section, from
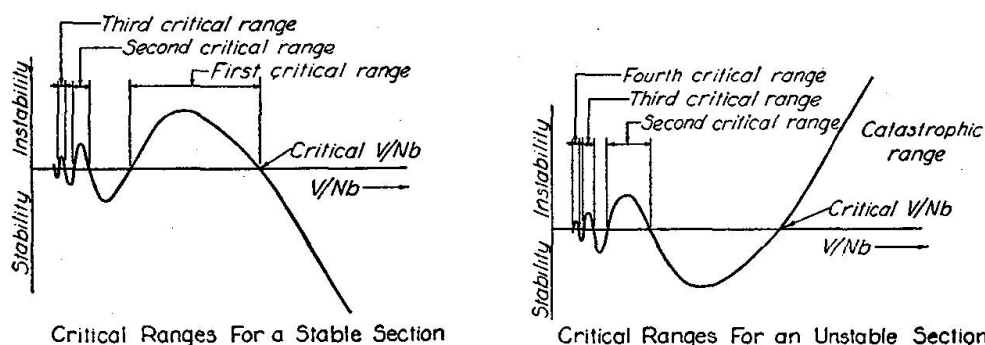

Fig. 9. Critical Ranges for Stable and Unstable Sections. Catastrophic Range in Unstable Sections and Lower Ranges of Minor Potential Oscillations.

zero at or near the leading edge, where the aerodynamic disturbance is initiated, to a maximum at the trailing edge, the total energy input over the section is obtained by integrating the expression of eq. (10) over the entire width. If the positive contributions of ΔW (representing energy input) dominate in the summation, the section will be *unstable*. If the negative contributions of ΔW (representing energy withdrawn) dominate in the summation, the section will be *stable* [5, 10, 12].

Accordingly, the stability or instability of a section depends not only upon the shape and proportions of the section but also upon a function of the wind velocity V. The over-all phase difference across the section, i. e., the fraction or multiple of a cycle required to traverse the width of the section, is

$$\frac{\phi}{2\pi} = \frac{Nb}{V} \tag{11}$$

where V is the horizontal velocity of the fluid flow, N is the frequency of the oscillations, and b is the width of the section. (Compare the Strouhal number, S.) Reciprocally, $V/(Nb)$ is the fraction or multiple of the width traversed per cycle. It is a convenient dimensionless ratio, commonly termed the "reduced velocity"; I refer to it as the "velocity ratio". All critical velocities and critical ranges of velocity are expressed in terms of $V/(Nb)$. A critical value of $V/(Nb)$ marks the lower limit of the catastrophic range (fig. 9) [10, 12].

As affecting the velocity ratio (V/Nb), infinite V or zero N represents the same limiting case of zero phase difference. This explains why stability or instability at very high fluid velocity V corresponds directly to stability or instability as given by the wind-tunnel test on a stationary model (zero N) [12].

The foregoing relations and conclusions, which I derived and predicted analytically, have now been confirmed experimentally by other investigators [19].

Angular Stability and Instability

When we pass from the elementary sections of narrow width to wider sections, such as H-sections having the proportionate ratios of actual bridge cross-sections, their potential *torsional* instability must be considered as well as their vertical instability. The foregoing classification is simply extended, as indicated in fig. 10. A wind inclined upward, represented by R, may produce a

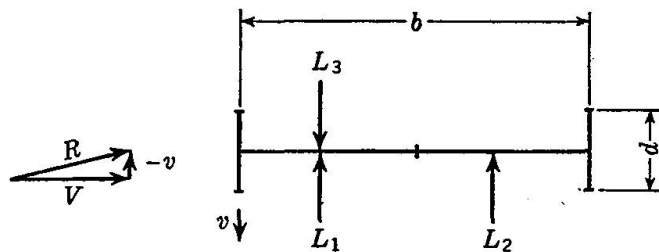

Fig. 10. Aerodynamic Instability of Wide Sections. Lift Resultants for Three Categories of Aerodynamic Stability.

resultant lift represented by L_1, L_2, or L_3, corresponding to three different categories of instability, as follows: L_1 (the ideal case), vertically and torsionally stable; L_2 (the most common case), vertically stable but torsionally unstable; and L_3 (the least common case), vertically and torsionally unstable. [5, 10] The proportions of the section (using the ratio of depth d to width b in the case of solid-web H-sections, and the reduced ratios of the equivalent H-sections in the case of open-web sections) determine the category of stability: L_1 for $d/b < 0.08$, L_2 for $d/b = 0.08$ to 0.24, and L_3 for $d/b > 0.24$ [12].

The static wind-tunnel graphs (fig. 8) will yield the same classification: L_1, positive slope of lift graph and of torque graph; L_2, positive slope of lift graph but negative slope of torque graph; and L_3, negative slope of both lift graph and torque graph. These classifications determine the basic stability or instability of the section with respect to vertical and torsional oscillations.

For the study of vertical oscillations, the foregoing concepts require no further modification or refinement. For the study of torsional oscillations, the foregoing concepts serve for preliminary classification and analysis, but are supplemented and modified for greater refinement by the additional concept of curved section models, presented below [10, 13].

Use of Stationary Section Models

By a principle of relativity, the motion of the section (regarded as an immersed boundary surface) may be translated into a relative tilt or distortion of the flow lines in the fluid, or into a contrary relative tilt or distortion of the boundary surface, so that in either case the boundary surface may then be treated (and tested) as stationary [10, 13].

For parallel *vertical* motion of the section with downward velocity v, the graphic representation (fig. 11) consists of the simple composition of horizontal flow lines with spacing $1/V$ and relative (upward) vertical flow lines with spacing $1/v$. By this graphic composition, the horizontal flow lines in the fluid are simply tilted up to a positive angle of incidence v/V. Instead of tilting the horizontal flow lines upward, an equivalent procedure is to tilt the section
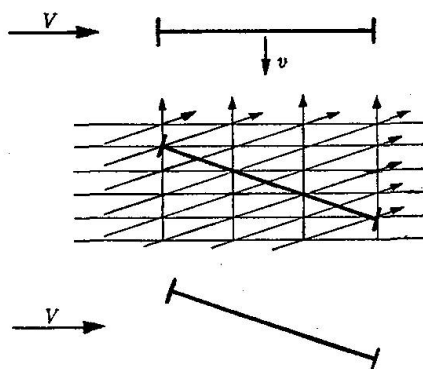

Fig. 11. Tilting of Field of Flow for Vertical Motion of Section. Tilting of Model in Static Wind-Tunnel Tests.

downward the same angle v/V; this is also given (fig. 11) by the graphic composition of the same superimposed flow lines with the direction of the vertical lines reversed. Accordingly:
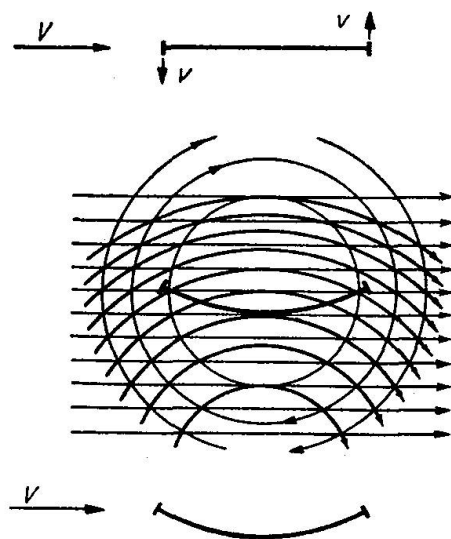
Fig. 12. Curving of Field of Flow for Angular Motion of Section. Derivation of Curved Models for Static Wind-Tunnel Tests.

Analogue 1. The *tilting* of the stationary model in a wind tunnel takes the place of a vertical velocity of the section.

When the same deductive procedure is applied to *angular* velocity of the section, the graphic representation (fig. 12) consists of the simple composition of the horizontal flow lines with spacing $1/V$ and a series of concentric circular flow lines with graduated spacing $\frac{1}{2}b/(cv)$, in which v is the linear downward velocity at the leading edge and c is the distance of any flow filament from the center. This graphic composition yields a series of concentric circular flow lines, convex upward. The angular velocity of the section is thus translated into a curved field of flow, as in an arching wind tunnel, with the immersed section model kept stationary and unchanged. Instead of curving the field of flow, an equivalent procedure is to curve the immersed section model an equal and opposite amount. This curvature is also given (fig. 12) by the graphic composition of the same superimposed flow lines with the direction of the rotational flow lines reversed. The equivalent warping of the immersed section model is symmetrical about the center of angular rotation, with horizontal tangent at this center and with slope change v/V at each end; the radius of curvature is $\frac{1}{2}bV/v$. Accordingly [13]:

Analogue 2. The *curvature* of the stationary model in a wind tunnel takes the place of an angular velocity of the section.

With a curved section model, as in the more familiar tilted section model, the added angle of incidence at the leading edge remains $-v/V$.

For wind-tunnel duplication of this condition, the section model must be warped to the circular (or parabolic) curvature defined above, with horizontal tangent at the center of rotation and the curvature changed for different desired values of the slope β at the leading edge (angle of incidence at the

leading edge equivalent to angular velocity of section). This curvature is called the "dynamic camber". A simple analytic derivation yields a parabola for the aerodynamic camber [15].

The first wind-tunnel tests on curved models of bridge sections were made for me in 1947 at the Virginia Polytechnic Institute by F. J. Maher [13].

In the absence of such tests on curved models, my analysis for the effect of angular velocity had previously been based on the static torque graphs obtained from straight section models (simply tilted instead of curved). Qualitatively, the results and conclusions are substantially unchanged, since the major disturbance of the incident stream flow is determined by the effective angle of incidence at the leading girder. Quantitatively, the correction from straight section models to curved section models is in the direction of reducing stability torque or intensifying instability torque [13].

It should be noted that the straight, tilted section model has a dual significance. It represents the effect of angular position, α, also the identical effect of vertical velocity, v. Accordingly, in aerodynamic formulas, the two are interchangeable; the conversion relation is simply $\alpha = -v/V$. The two contributions may be bracketed, as $(\alpha - v/V)$, with the same factors and coefficients applied to both.

The curved section model represents solely the effect of angular velocity, $\dot{\alpha}$. The conversion relation is $\beta = -v/V = -b\dot{\alpha}/(2V)$.

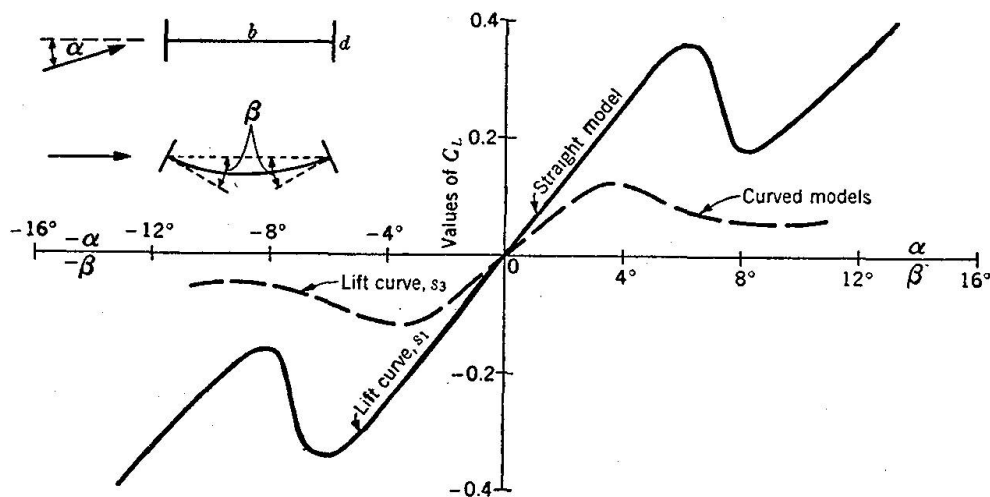Fig. 13. Static Lift Graphs for Straight and Curved Models of an H-Section ($d/b = 0.20$).

Fig. 13 shows the static *lift* graphs obtained from straight and curved section models, respectively, for an H-section of section ratio $d/b = 0.20$ (approximately the section of the original Tacoma Bridge) [13].

Fig. 14 shows the static *moment* graphs obtained from the same straight and curved section models [13].
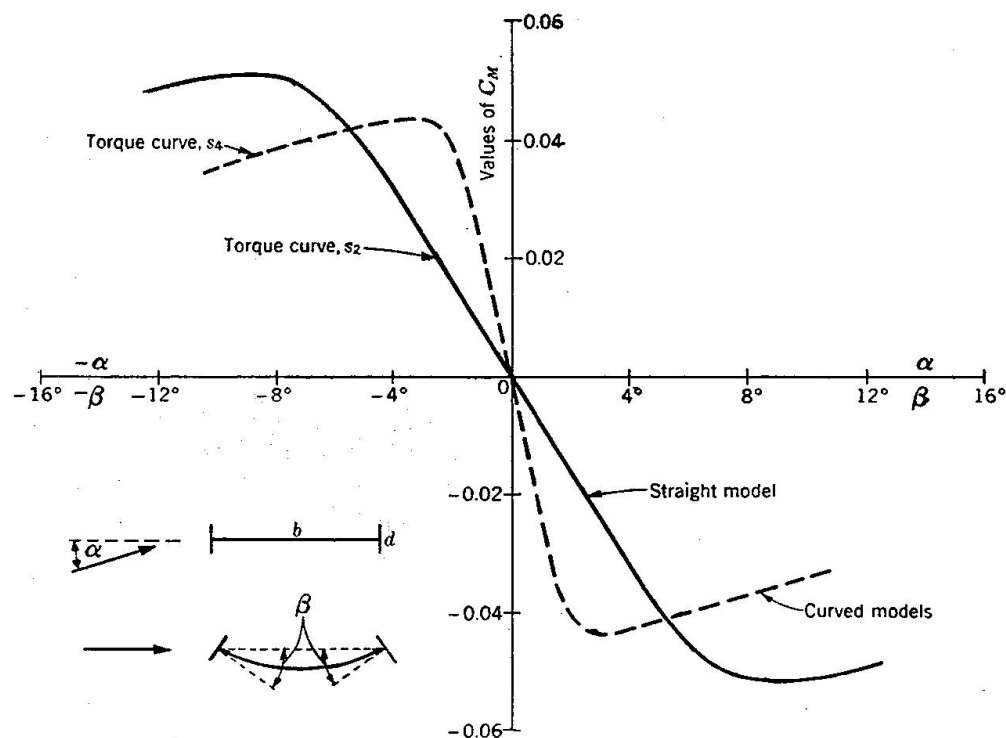
Fig. 14. Static Torque Graphs for Straight and Curved Models of an H-Section ($d/b = 0.20$).

Pressure Variation Across the Section

The curves of pressure distribution across the width of the section may be obtained experimentally by manometer readings on the stationary section model in the wind tunnel. Such graphs, plotted from tests made for me in 1947 by Dr. HUNTER ROUSE in a miniature wind tunnel at the Iowa Institute of Hydraulic Research, are shown in figs. 15 and 16 [10]. The integration or
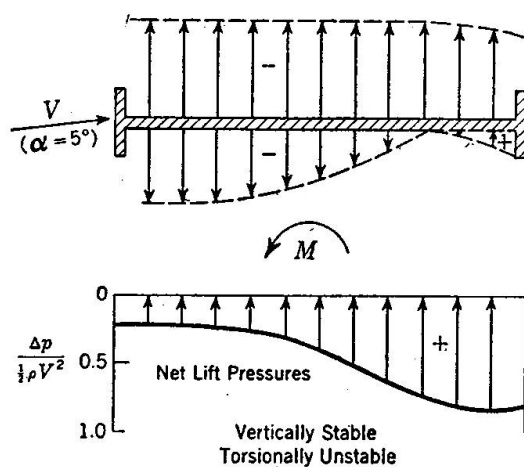

Fig. 15. Aerodynamic Pressure Distribution on an H-Section ($d/b = 0.16$). (Section Vertically Stable and Torsionally Unstable.)
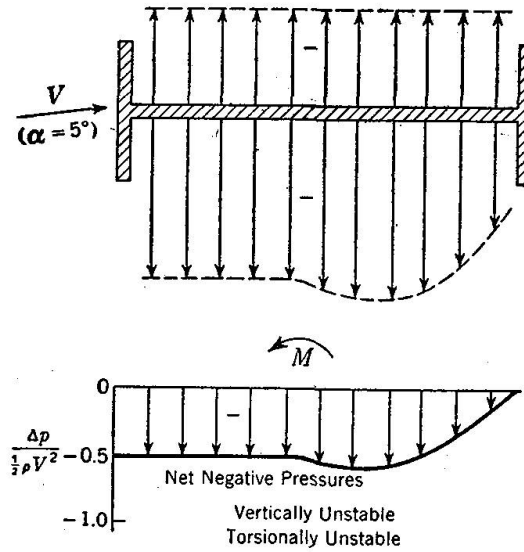
Fig. 16. Aerodynamic Pressure Distribution on an H-Section ($d/b = 0.33$). (Section
Vertically and Torsionally Unstable.)

algebraic summation of the *pressures* over the total width b gives the positive
or negative lift L, which checks the value given by the ordinate of the static
lift graph (after correcting for the drag component). Similarly the integration
or algebraic summation of the *moments* of these pressures about the center of
rotation gives the positive or negative torque M, which checks the value given
by the ordinate of the static moment graph. The direction and the point of
application of the resultant L of the graph of net lift pressures may be compared
with the identification of the different categories of aerodynamic instability,
assembled in fig. 10 [14].

Prediction of Aerodynamic Behaviour of Bridges

My analysis is reduced to very simple working formulas for predictively
computing the instability response curves of any given bridge cross-section for
all wind velocities [14].

For *vertical* instability,

$$\delta_1 = 0.02\, B \cdot A\, \frac{V}{Nb} \tag{12}$$

where B is the (constant) width-factor of the section ($B = b^2/w$) having a mean
normal value of 0.25 (in units of feet and pounds); $V/(Nb)$ is the relative wind
velocity, that is, the velocity measured with the width b as the unit of length
and the period of oscillation ($1/N$) as the unit of time; and A is the (variable)
aerodynamic factor, also given by a very simple formula:

$$A = -\int_0^1 p \cdot \cos\phi \cdot dx \tag{13}$$

where the integration extends over the width of the section. Here p is the variable ordinate of the pressure distribution curve (figs. 15, 16) per unit angle of incidence; and the multiplier cos ϕ is the correction for phase difference, as explained above. The phase difference ϕ increases in a straight-line ratio from zero at the leading edge to a maximum of $\phi_1 = Nb/V$ at the far edge of the section, so that $\phi = x \cdot \phi_1$. This correction factor for *phase difference*, introduced by me, is significant. It explains the otherwise mystifying variation of aerodynamic response at different wind velocities [12, 14].

Fig. 17. Vertical Instability Graphs for Three H-sections. Stable Section, $d/b = 0.16$; Neutral Section, $d/b = 0.24$; Unstable Section, $d/b = 0.33$.

In fig. 17 are plotted the *vertical* instability graphs computed for three different H-sections: a *stable* section ($d/b = 0.16$), a *neutral* section ($d/b = 0.24$), and an *unstable* section ($d/b = 0.33$). These curves are computed directly from the respective pressure-distribution curves, figs. 15, 16, using the simple integration formula, eq. (13). The abscissas are the relative velocities V/Nb and the ordinates are the coefficients of aerodynamic instability, AV/Nb, the variable term of eq. (12) [14].

A section is here termed vertically or torsionally *stable, neutral,* or *instable* to designate its aerodynamic response at high wind-velocities, in the critical high-velocity or "catastrophic" range. The same sections will usually have *minor* alternating ranges of stability and instability at low wind velocities, as shown in the calculated response graphs illustrated by fig. 17 [12, 13, 14].

For the section ratio 0.16, the graph shows assured vertical *stability* in the high velocity range, above a critical V/Nb of 2.7. Above this value, any increase in wind velocity V makes the bridge more stable, quickly damping any initiated oscillations. Below this velocity-ratio there is a range of limited instability, preceded by minor alternating ranges at lower velocities. These minor instability ranges explain the vertical oscillations of the Tacoma Bridge at low wind velocities.

For the section ratio 0.33, the graph shows a *catastrophic* range of vertical *instability* starting at a critical V/Nb of only 1.40, with minor alternating ranges at lower velocities.

For *torsional* instability (before correction for curved section models), the logarithmic increment is given by [14]

$$\delta_2 = 0.02 \frac{b^2}{2\,r^2} \cdot B \cdot A \frac{V}{Nb} \qquad (14)$$

Here only one factor is added to eq. (12), namely $b^2/2\,r^2$, with a mean normal value of 4.0, where r is the polar radius of gyration of the mass of the cross-section; and the formula for A becomes

$$A = -\int_0^1 p\left(\tfrac{1}{2}-x\right)\cos\phi \cdot dx \qquad (15)$$

with the new factor $(\tfrac{1}{2}-x)$ representing the lever arm of each ordinate about the center.

In fig. 18 are shown the *torsional* response graphs computed by eq. (15) for three different sections [14].

For the section ratio $d/b = 0$ (a flat plate), the graph shows assured *torsional stability at all wind velocities.* (This section is also *vertically* stable at all wind velocities. The only possible instability is that of *coupled* vertical and torsional oscillations; the analysis for this condition has also been published by me [13].)

For the section ratio 0.16, the graph (fig. 18) shows a steep *catastrophic* range (like that which destroyed the Tacoma Bridge), starting at a critical V/Nb of 4.0, with alternating ranges of stability and minor instability at lower velocities.

For the *neutral* section ratio 0.08, the graph shows assured *stability* at all velocities above a low critical V/Nb of 1.0, with minor humps at lower velocities, representing negligible instability that is easily overtopped by normal structural damping. In this case, the asymptotic range for the neutral section is below the
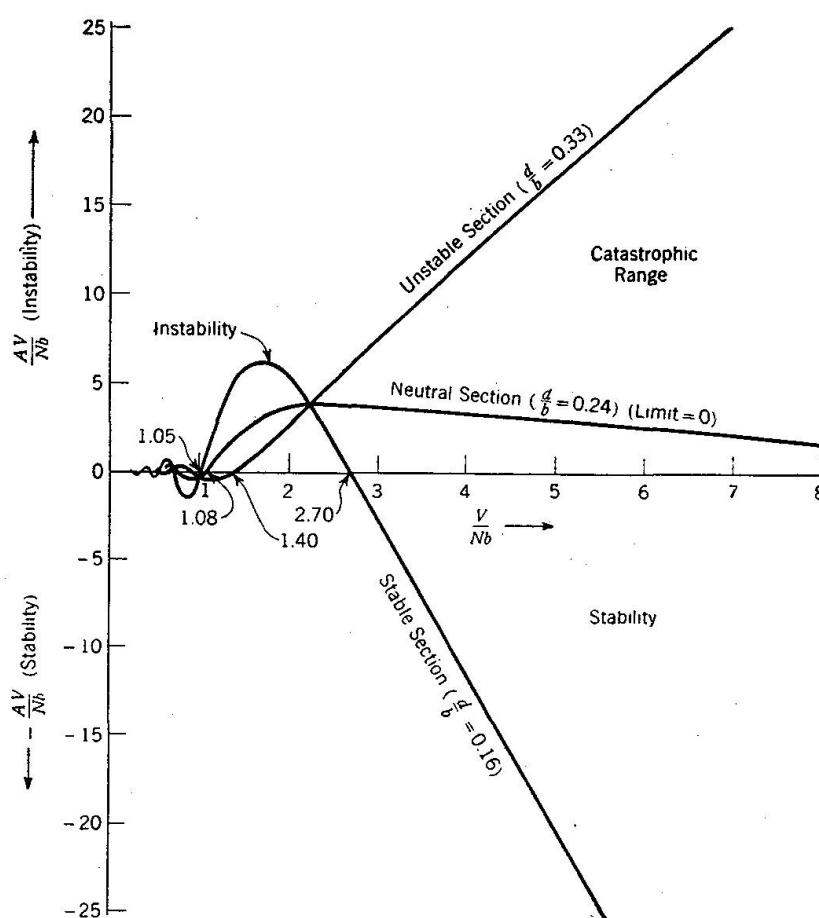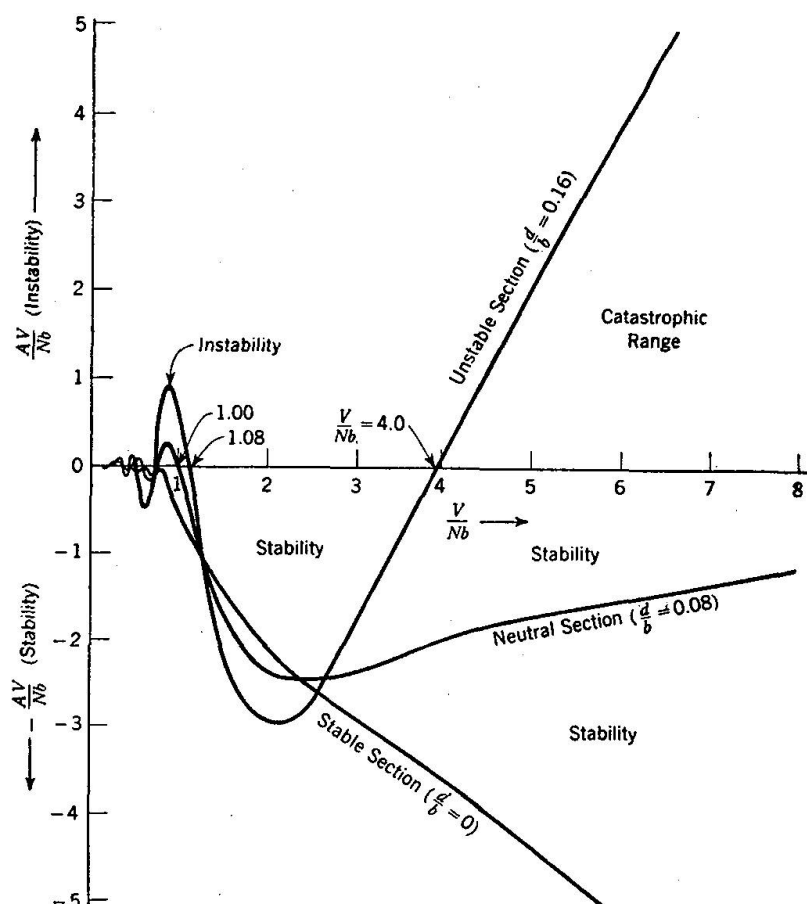
Fig. 18.   Torsional Instability Graphs for Three H-Sections. Stable Section, $d/b = 0$; Neutral Section, $d/b = 0.08$; Unstable Section, $d/b = 0.16$.

axis, representing stability, whereas in fig. 17, it was above the axis, representing (limited) instability.

It is possible to get the answer, with sufficient accuracy for all practical purposes, without requiring pressure-distribution curves. An alternative method of deriving and plotting the aerodynamic response curves is to use the simple static lift and torque graphs of the section [15].

Valuable series of such graphs, for H-sections and for deck sections, also for various modified sections, have been obtained for me and generously contributed by Prof. F. J. MAHER, using the wind tunnel at Virginia Polytechnic Institute. In figs. 19 and 20 are assembled typical lift and torque graphs, respectively for H-sections. The slopes (angular gradients) of these graphs, at any angle of incidence, provide the criterion and the measure of aerodynamic stability [15, 16].

If s_1 is the slope of the lift graph and s_2 the slope of the torque graph, s_1 is a measure of the lift resultant on the section, and $e = s_2/s_1$ is the eccentricity of the resultant, its distance from the center line [15].
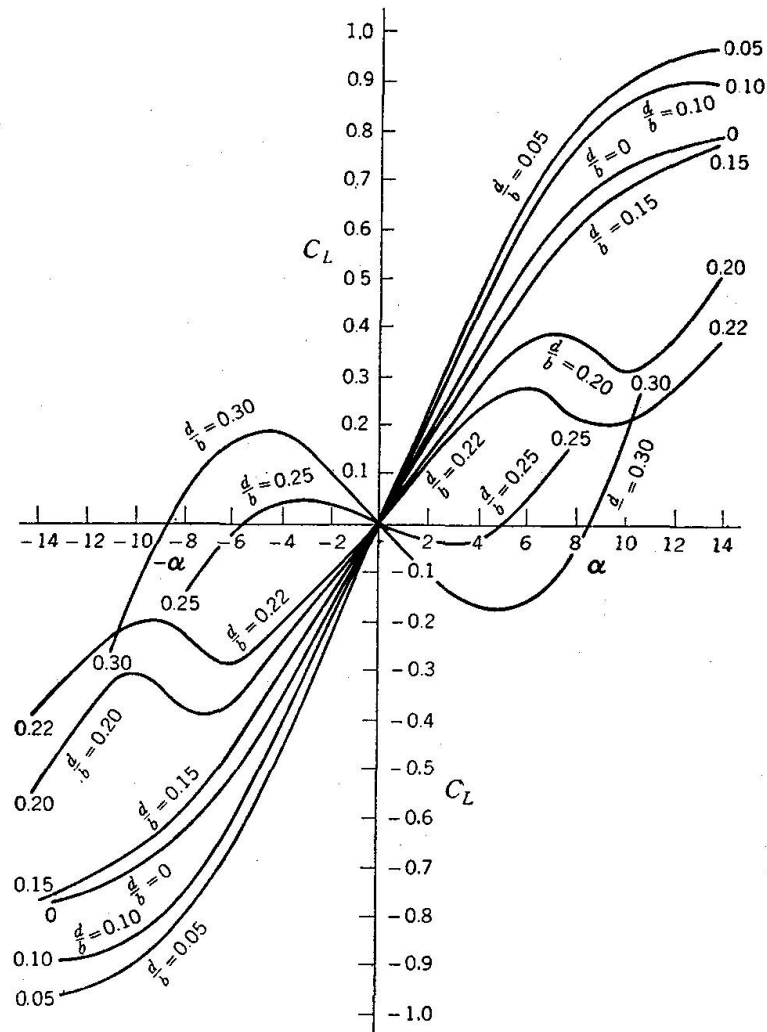
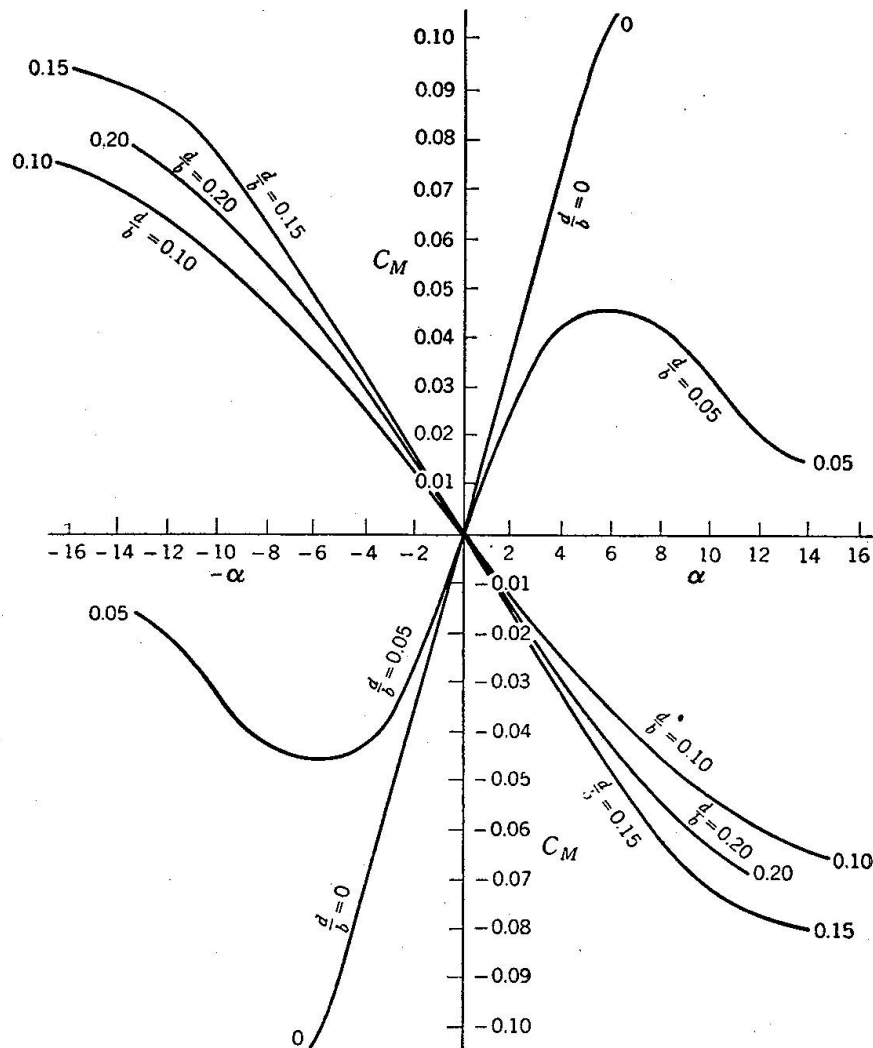Fig. 19. Typical Static Lift Graphs of H-Sections ($d/b = 0$ to 0.30).

Assuming a straight-line pressure distribution across the width of the section, the end ordinates p_0 and p_1 are given by the simple relation

$$p_0 = s_1 + 6\,s_2, \quad p_1 = s_1 - 6\,s_2 \tag{16}$$

If this straight-line graph of p is used in eqs. (13) and (15) instead of the actual pressure-distribution curves illustrated in fig. 15 and 16, almost identical results are obtained yielding aerodynamic response graphs sufficiently accurate and informative for all practical purposes. In fig. 21 I give a comparison of the torsional instability graphs computed by the two methods (using the two different kinds of test data from two different laboratories) for an H-section of $d/b = 0.16$. For practical purposes, the difference is negligible [15].

General Aerodynamic Equations for Oscillating Sections

By rigorous mathematical analysis applied to basic physical concepts, I have derived the following general aerodynamic equations for the forces (L and M) acting on any moving or oscillating section in any relative fluid flow [13].

Fig. 20. Typical Static Torque Graphs of H-Sections (d/b = 0 to 0.20).

Fig. 21. Comparison of Instability Graphs for an H-Section (d/b = 0.16) by Exact and Approximate Methods.

$$L = L_0 + \tfrac{1}{2}\rho\,V^2 b\left[C_1 s_1\left(\alpha - \frac{\dot\eta}{v}\right) - C_3 s_3\frac{(b\,\dot\alpha)}{2V}\right] + m_a\,(V\,\dot\alpha - \ddot\eta) \qquad (17\,\mathrm{a})$$

$$M = M_0 + \tfrac{1}{2}\rho\,V^2 b^2\left[C_2 s_2\left(\alpha - \frac{\dot\eta}{v}\right) - C_4 s_4\frac{(b\,\dot\alpha)}{2V}\right] - I_a\,\ddot\alpha \qquad (17\,\mathrm{b})$$

where L_0 and M_0 are the initial static lift and torque for the section at rest at the initial angle of incidence; $\dot\eta$, $\ddot\eta$, are vertical velocity and acceleration; α, $\dot\alpha$, $\ddot\alpha$, are angular displacement, velocity, and acceleration; s_1 and s_2 are the slopes of the static lift and torque graphs for the ordinary *straight* model; s_3 and s_4 are the slopes of the static lift and torque graphs for the *curved* model; m_a and I_a are the mass and the polar moment of inertia of the cylinder of air enveloping the section; and C_1, C_2, C_3, C_4 are phase-correction factors for the effect of time lag between any change in attitude or motion of the section and the resulting pressures across the width of the section. All moments are taken about the midpoint of the width b [13].

Eqs. (17) are of fundamental importance. They are the pivotal formulas of the analysis presented. The applicability of eqs. (17) is without restriction as to the nature of the motion or oscillation of the section (uniform, irregular, or harmonic). Moreover, the section may be horizontally stationary in a steady wind (as in the case of a bridge) or moving horizontally relative to the wind (as in the case of an airplane); V is the relative wind velocity.

In the case of harmonic oscillations, the coefficients C_1, C_2, C_3, and C_4 are functions of the velocity ratio $\frac{V}{Nb}$ $\left(\text{or of } k = \frac{\omega b}{2V} = \frac{\pi Nb}{V}\right)$. In such case, the C-coefficients are of the vector form, $C = F - i\,G$, representing an angle of lag equal to $\tan^{-1} G/F$. The values of F and G may be calculated and plotted from the pressure distribution graphs for the section (F_1, F_2, G_1, and G_2 from the straight model; F_3, F_4, G_3, and G_4, from the curved model) [13].

In eqs. (17) all the terms and parameters within the brackets are dimensionless. The outside terms may also be written in terms of $\rho\,V^2 b$ or $\rho\,V^2 b^2$ and dimensionless factors.

The ordinates of the pressure distribution graphs are designated by y_1 for the straight model and y_3 for the curved model. Each pressure ordinate, y_1, or y_3, lags an amount ϕ behind the respective displacement or velocity vector that produces it.

For each force or moment vector Cs, Fs is the cosine component and $-i\,Gs$ is the sine component. The angle of lag of the resultant force or moment vector is $\tan^{-1}(G/F)$. Accordingly, for the force vectors,

$$F_1 = \frac{\int_0^1 y_1 \cos\phi\,dx}{\int_0^1 y_1\,dx\,(= s_1)}\,; \qquad G_1 = \frac{\int_0^1 y_1 \sin\phi\,dx}{\int_0^1 y_1\,dx\,(= s_1)} \qquad (18\,\mathrm{a})$$

with similar expressions for F_3 and G_3; and, for the moment vectors,

$$F_2 = \frac{\int_0^1 y_1(\tfrac{1}{2}-x)\cos\phi\,dx}{\int_0^1 y_1(\tfrac{1}{2}-x)\,dx\,(=s_2)}; \qquad G_2 = \frac{\int_0^1 y_1(\tfrac{1}{2}-x)\sin\phi\,dx}{\int_0^1 y_1(\tfrac{1}{2}-x)\,dx\,(=s_2)} \tag{18b}$$

with similar expressions for F_4 and G_4 [13].

The F-graphs and G-graphs for any section, as functions of V/Nb, are computed by eqs. (18) from the pressure distribution graphs. The computation and plotting of the graphs are expedited by the use of an electric analogue computer.

Equating the *aerodynamic* forces given by eqs. (17) with the *dynamic* resisting forces given by the general dynamic equations for oscillating sections, the general *force* equations for an oscillating section are obtained. These general force equations (not reproduced here) are the key equations for solving the various problems of aerodynamic oscillations [13].

For pure vertical oscillations, the general force equations yield the rate of amplification:

$$\delta_1 = -\frac{\mu}{4}\,(F_1 s_1)\,\frac{V}{Nb} \tag{19}$$

which is identical with eq. (12); also with eq. (9), with the factor F_1 here added for phase correction.

For pure angular oscillations, the general force equations yield the rate of amplification:

$$\delta_2 = -\frac{\mu b^2}{8 r^2}\left(\frac{G_2}{k} s_2 + F_4 s_4\right)\frac{V}{Nb} \tag{20}$$

which is the final corrected form of eq. (14).

Eqs. (19) and (20) yield the instability-response curves, which may thus be plotted predictively for varying V/Nb [13].

By writing the equations of the static lift and torque graphs in general form and substituting the resulting mean effective values of the slopes s_1, s_2, s_3, s_4, in eqs. (19) and (20), equations are obtained for determining the *limiting* vertical and angular amplitudes with varying velocity ratio V/Nb. Numerical and graphic solutions are supplied for predictively plotting the amplitude-response curves [13].

From the general force equations, I have also derived the complete solution for *coupled* vertical and torsional oscillations, corresponding to the dangerous "flutter" of airplane wings and control surfaces. A typical instability- response graph computed, by my formulas for coupled oscillations, for a real section ($d/b = 0.02$) is shown in fig. 22 [13].

The analysis I have developed, as herein outlined, is believed to be the first generalized aerodynamic theory of oscillating sections, not limited to sections of any one type. It also constitutes the aerodynamic theory of bridge oscillations brought to greater completeness and generality than any previously attempted.
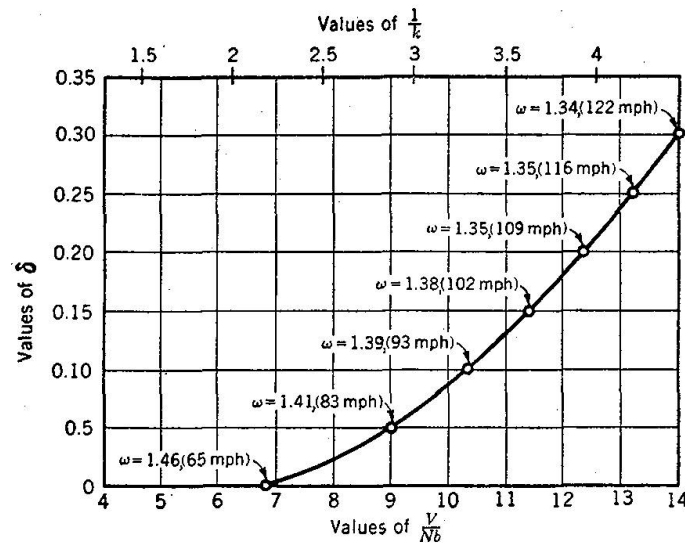
Fig. 22. Instability Graph for Coupled Vertical and Torsional Oscillations. Showing Logarithmic Increment (δ) and coupled Frequency (ω) for Varying Wind Velocities (V/Nb), and Critical Velocities (V/Nb) for Varying Structural Damping (δ). (For Section $d/b = 0.02$.)

It is believed to be the first complete theory of aerodynamic oscillations with the following features of distinguishing generality [13]:

1. It is not limited to streamline airfoil sections and idealized thin plates but is also applicable to all bridge sections or other sections of whatever type or form.

2. It is not limited to coupled oscillations (as in airplane flutter) but also covers vertical oscillations and torsional oscillations (which are the known forms of bridge instability).

3. It is not limited (like prior aerodynamic theory) to predicting critical flutter velocity but also determines and predicts all critical wind velocities for vertical and torsional oscillations and, in addition, rate of amplification, limiting amplitudes, and amplitude response at all wind velocities.

4. It does not require, for each problem, large-scale oscillating model tests, which are costly and time-consuming, but instead determines all necessary constants for any section by simple static tests on small-scale section models.

Criteria for Assuring Aerodynamic Stability [1, 12]

In the absence of scientific design to improve the aerodynamic characteristics of the cross section and in the absence of other means of stabilization or stiffening, aerodynamic stability can be secured by simply providing adequate depth of stiffening trusses or girders. As a first criterion to apply, I have derived and established the following simple specification:

Specification 1. The depth of stiffening trusses or girders shall be not less than $l/120 + (l/1000)^2$, *unless aerodynamic stability is otherwise assured* [12].

For the Tacoma Bridge span of 2800 feet, the foregoing specification would have required a depth of 31 feet, or 1 : 90 of the span. The stiffening girders of the original Tacoma Bridge were made 8 feet deep, or only 1 : 350 of the span. It was by far the most flexible suspension bridge of modern times.

In suspension bridges with generously proportioned stiffening trusses, a shallower depth ratio than specified above will yield the requisite stiffness and damping. If the foregoing first criterion is not satisfied, the next test to apply is my more general specification:

Specification 2. The stiffening system of a suspension bridge shall have a value of EI of not less than $b\,l^4/60\,\sqrt{f}$, unless aerodynamic stability is otherwise assured [12].

If the foregoing tests, easily applied, are not satisfied, a more intimate examination of the aerodynamic constants of the structure is required. Any deficiency may be made up by special provisions or corrected by special design.

The most important constant in aerodynamic studies for any structure is the "spring constant" or *coefficient of rigidity* K. It measures the resistance to oscillation and determines the natural period or frequency of harmonic oscillations in any mode. The numerical value of K can be easily and accurately calculated for any existing or proposed structure of known dimensions. The mode $n = 2$ (the main span oscillating in two segments with a node at mid-span) is most conveniently used for calculating K, since the fundamental mode ($n = 1$) will rarely give a value materially lower. For all even values of n (the anti-symmetric modes), K is given quickly, scientifically, and precisely by my simple formula [12]

$$K = \frac{\pi^2 n^2}{l^2} H + \frac{\pi^4 n^4}{l^4} EI \qquad (21)$$

where H is the horizontal component of dead-load cable stress. This value of K for $n = 2$ ranges from 124 in the ill-fated Tacoma span to 2164 in the Williamsburg Bridge. Low values of K are associated with aerodynamic instability; but K alone does not tell the whole story.

The two terms in the above formula for K (the H term and the EI term) represent the contributions of the cables and the stiffening girders, respectively. The ratio of the girder term to the total is the stiffening ratio R, and largely determines the structural damping. The value of R ranges from 0.015 in the collapsed Tacoma span to 0.780 in the Williamsburg Bridge. Low values of R (below 0.25) are associated with aerodynamic instability [7, 12].

Another important dimensional constant is the width factor B ($= b^2/w$) in which w is the weight of the span per linear foot. Aerodynamic instability increases with the square root of B. The value of B (with w per full width) is fairly constant at approximately 0.25 for most suspension bridges. For wide bridges of normal or reduced weight per square foot, the value of B is greater, even doubled, as in the Bronx-Whitestone Bridge, thereby adding 41% to the

instability. Contrary to popular misconception, the *narrowness* of the Tacoma Narrows Bridge was not the cause of its failure. (The name of the bridge may have subconsciously contributed to this hasty, erroneous conclusion.) If the bridge had been wider, it would have been more vulnerable to aerodynamic action, with more rapid amplification and greater amplitudes; and its instability would have been more difficult to counteract or cure [12].

All formulas for aerodynamic instability contain the dimensional factor $\sqrt{B/K}$. The three measures of instability are rate of amplification, critical velocities (in the catastrophic range), and maximum amplitudes. Considerations of all three measures yield the same conclusion [12]:

> *Safety against aerodynamic instability is proportional to* $\sqrt{K/B}$.

This relation yields a simple criterion, of rational form on a statistical base, for quickly checking the aerodynamic stability of a proposed bridge design:

> *Criterion 1.* The rigidity ratio K/B shall exceed 1200 (unless aerodynamic stability is otherwise assured) [12].

The values of K/B range from 468 for the Tacoma span to 16,028 for the Williamsburg Bridge. No bridges with a K/B greater than 1200 have ever, as far as known, shown any traces of aerodynamic instability. On the other hand, all bridges with a K/B less than 1200 have evidenced aerodynamic instability, in varying degrees.

A more accurate and more discriminating criterion, taking into account the variation in structural damping represented by the stiffening ratio R, may also be simply stated:

> *Criterion 2.* The aerodynamic stability constant $R \sqrt{K/B}$ shall exceed 10 unless aerodynamic stability is otherwise assured) [12].

The values of $R \sqrt{K/B}$ range from 0.4 for the Tacoma span to 100 for the Williamsburg Bridge. All bridges with values for $R \sqrt{K/B}$ of less than 10 have been subject to aerodynamic oscillations. All bridges with this constant greater than 10 have been aerodynamically stable.

A still more scientific criterion, more discriminating in borderline cases and safer to use in abnormal cases, takes into account the variation of potential instability with the form and proportions of the cross-section. For different section-ratios d/b I have plotted and tabulated the formula values of potential torsional and vertical instability (δ). The formula value of the positive damping (δ_s) for any given structure or design is then compared with the corresponding recorded value of maximum δ. The ratio is the *factor of safety against aerodynamic instability*.

This ratio varies from 0.02 in the Tacoma span to 5.3 in the Williamsburg Bridge. All bridges for which this ratio is less than *unity* have been subject to aerodynamic oscillations, with a highly consistent order of vulnerability and

seriousness; and all bridges for which this ratio is greater than unity have been aerodynamically stable [7, 12].

From my formulas and wind-tunnel data, I have plotted a graph to facilitate this comparison. All bridges whose plotted points fall below the instability curve are in the unstable category, and those whose plotted points fall above the curve are in the stable classification. Degree of stability (or factor of safety) is represented by the ordinate of the plotted point divided by the corresponding ordinate of the graph. This comparison, expeditious but comprehensive, is represented by my third criterion for aerodynamic stability:

> *Criterion* 3. The aerodynamic stability constant $R \sqrt{K/B}$ (or the value of $\delta_s \sqrt{K/B}$ which it represents) shall exceed the required value for the section, as tabulated or as plotted in a graph for different section ratios and forms of section [7, 12].

We thus have two simple, practical specifications and three alternative criteria, of progressively increasing scientific accuracy, to aid in quickly checking the aerodynamic stability of a proposed bridge design.

Here at last is an answer to the question that has challenged bridge engineers for a century: *How much stiffening does a suspension bridge require?* Any suspension bridge with a stiffening system satisfying specification 1, or specification 2, or criterion 1, will be aerodynamically stable. If the EI provided by the stiffening girders or trusses does not satisfy specification 2, additional stiffening must be provided by means of stays or other means to satisfy criterion 2; otherwise the section must be modified to eliminate or reduce the aerodynamic instability until criterion 3 is satisfied [1, 2, 4, 7, 12].

It should be noted that the alternative specifications 1 and 2 are so worded as not to freeze progress but to encourage initiative and reward resourcefulness and scientific design [7, 12].

Prevention and Cure of Aerodynamic Instability

The Tacoma Bridge disaster has awakened the profession to one important lesson: *Designers of suspension bridges must henceforth give consideration to the aerodynamic stability of their structures.*

John A. ROEBLING, in his writings and in his work (1840—1869), was the first bridgebuilder to recognize the problem of aerodynamic stability; without the benefit of modern scientific and mathematical knowledge but with intuitive perception, he built his spans with special provisions to stiffen them and make them aerodynamically safe. But subsequently, for three-quarters of a century, this phase of the bridge engineer's problem completely dropped from sight. We now have had to pick up the problem where ROEBLING left it and, with far more mathematics and science than he had available, to carry the solution to maximum completeness and practical applicability [4, 6].

It is of course easy, especially in the shorter spans, to assure aerodynamic

safety by generous stiffening, disregarding economy and appearance. The real problem, however, is to assure aerodynamic stability without wasting material on excessive stiffness and without sacrificing artistic proportions.

The principal lines of attack for securing or improving aerodynamic stability are the following [6]:

1. To augment the rigidity of the structure.
2. To augment the positive damping.
3. To modify the cross-section.

For *resistance* to aerodynamic effects, the most significant constants of the structure are the coefficient of rigidity K and the stiffening ratio R (the ratio of the contribution of the stiffening elements — trusses, girders, stays, etc. — to the total rigidity). The magnitude of R largely determines the structural damping [12].

Almost any method of increasing rigidity is also directly effective in augmenting structural damping. Rigidity and structural damping to resist potential aerodynamic instability, both *vertical* and *torsional*, may be augmented, in precalculated amounts, by using: deeper stiffening girders or trusses; cable stays, tower stays, center stays, and intermediate stays; continuous construction, and straight backstays. In addition, rigidity and structural damping to resist potential *torsional* instability may be augmented in precalculated amounts by using transverse diagonal stays; installing a double (top and bottom) system of lateral bracing; increasing the torsional stiffness of the towers; raising the points of suspender connection; and lowering the center of gravity of the section (for example, by placing the roadway at the bottom) [6, 12].

In amplitudes attainable, magnitude of kinetic energy accumulated, and structural strains produced, *two-segment* (single-node, or $n = 2$) torsional oscillations are generally the most dangerous potential manifestation of aerodynamic instability — as in the case of the Brighton Chain Pier (1836) and the Tacoma Bridge (1940). A highly effective method of curing, preventing or resisting such two-segment torsional oscillations is to provide adequately proportioned center stays (fig. 23) or other equivalent means of preventing relative longitudinal motion of cable and suspended structure at midspan. Such center stays were first conceived and applied by me on three suspension bridges in 1938, and were promptly presented by me to the profession in a published paper and at a professional meeting.

Another economical method is to use longitudinal diagonal stays, inclined in either direction, in the planes of the cables (fig. 24). Such stays may be located either above or below the roadway, and may have their points of attachment to selected points of the cable, or to points of the stiffening girder, or to both. ROEBLING developed and applied this concept in his suspension bridges. The first modern application was made by me on three suspension bridges in 1938, and this was promptly presented to the profession.
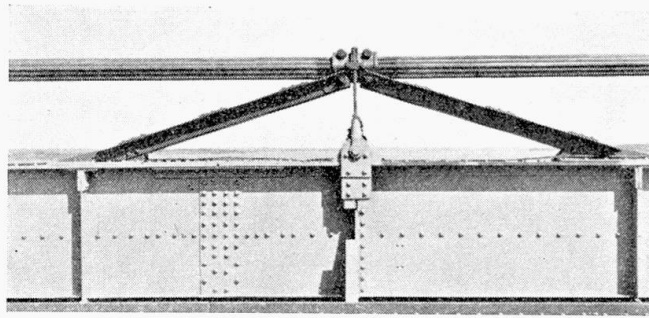
Fig. 23. Mid-Span Stays for Preventing Torsional Oscillations. Installation on Thousand Islands Bridge and Deer Isle Bridge, 1938.
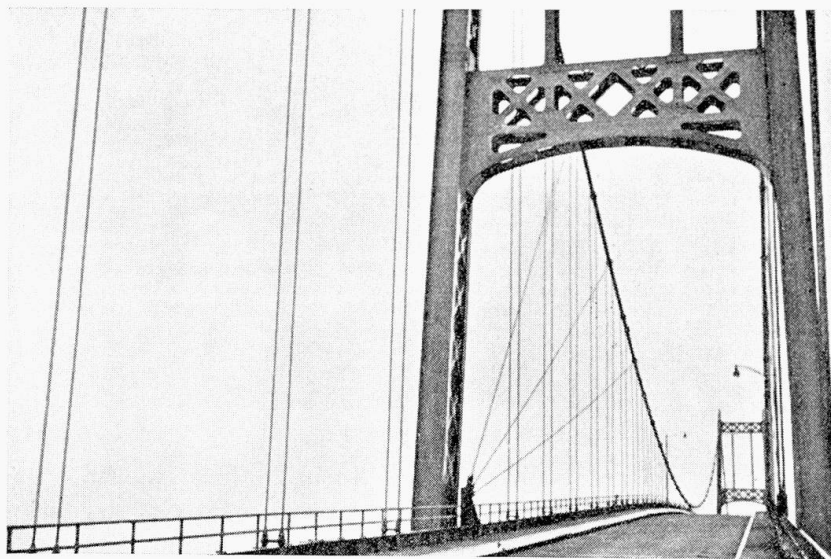

Fig. 24. Cable Stays for Checking Aerodynamic Oscillations. Installation on Thousand Islands Bridge and Deer Isle Bridge, 1938.

For maximum effectiveness, the two types, cable stays and tower stays, may be combined to form a double system. In the case of the Tacoma Bridge, such a double system near each end of the span, as calculated by me, would have increased K from 124 to 1204, at the same time raising the value of R from the very low value of 0.015 to the extremely high value of 0.900. This would have brought the aerodynamic constants of the Tacoma span to very generously safe values [6, 12].

The most advanced development of my use of cable stays is embodied in my design for the proposed Messina Straits Bridge, to link Sicily to Italy, with a main span of 5,000 feet, to be the longest span in the world (fig. 25). Here a beautiful system of radiating cable stays is incorporated in the design as a scientifically calculated feature to prevent oscillations and assure aerodynamic stability [17].
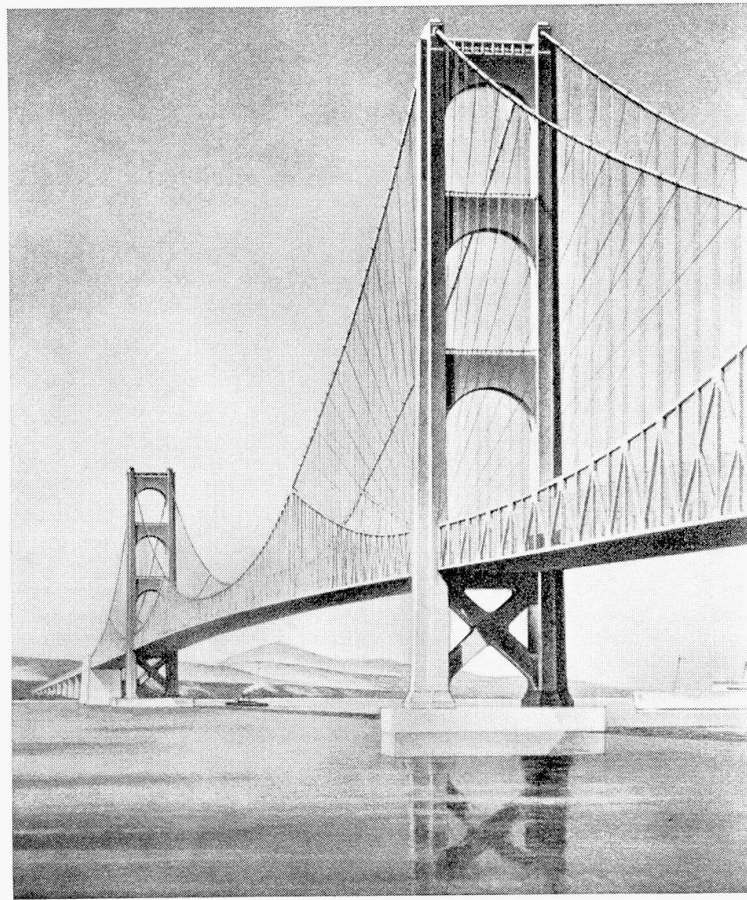
Fig. 25. Messina Straits Bridge, to Link Sicily to Italy. Main Span of 5,000 feet, to be the Longest in the World. Rigid Type of Stiffening Truss and System of Radiating Cable Stays to Assure Aerodynamic Stability. (Designed by the Author.)

Fig. 26. Intermediate Stays for Checking Aerodynamic Oscillations. Installation on Deer Isle Bridge, Maine, 1943.
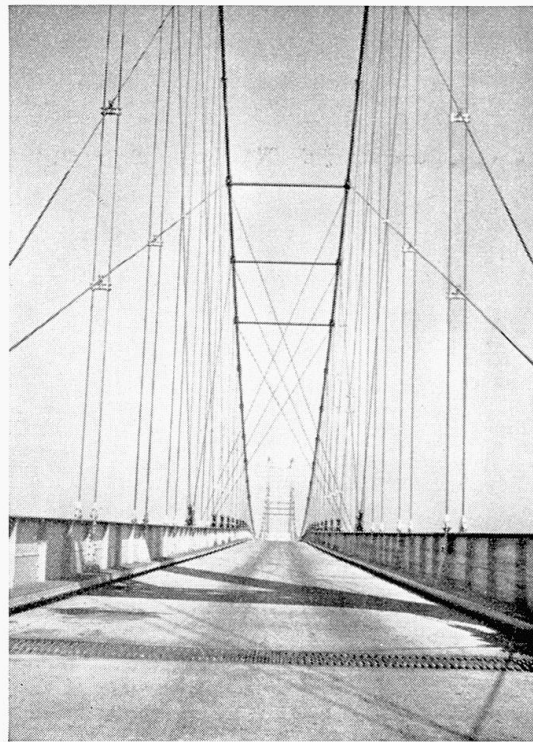
Fig. 27. Transverse Diagonal Stays to Prevent Torsional Oscillations. Installation on Deer Isle Bridge, Maine, 1943. Three Pairs of Transverse Stays Near the Quarter Point. Top Strut Added for Greater Effectiveness.

For stiffening a flexible design, the cable stays at the ends of the span and the center stays at midspan may be supplemented by a system of intermediate stays, also in the plane of the cable (fig. 26). My formulas provide for their scientific design to provide any desired increase in the value of K [6, 12].

In addition or as an alternative to the longitudinal diagonal stays, an economical and strikingly effective method of curing or preventing torsional oscillations is the use of *transverse* diagonal stays (fig. 27) located between opposite suspenders at selected points of the span. Transverse horizontal struts or ties between the cables may be used in conjunction with such stays for still greater effectiveness. For the Tacoma span, diagonal stays of only 1 sq. in. per panel point would have yielded a more than 50-fold augmentation in *torsional* resistance, represented by an increase in K from 124 to 7064 — many times more than sufficient for assured torsional stability. The Deer Isle Bridge (on the Maine coast) has been equipped by me with such a system as a safety precaution, to preclude any possibility of torsional oscillations developing at wind velocities higher than the 80-mile storms thus far experienced at this coastal location [6, 12].

Another highly effective method of augmenting resistance to torsional oscillations is by providing two planes of lateral bracing, at or near the top and bottom flanges of the stiffening girders (or trusses), respectively, so as to secure the integral effect of a hollow rectangular section in torsion. According to my

formulas, as applied to the Tacoma span, by adding comparatively light systems of top and bottom lateral bracing (5 to 20 sq. in. of equivalent horizontal web section), K is increased from 100 to 400 percent, and R is multiplied $35-$ to $50-$ fold (which means a corresponding increase in the structural damping). The higher values of K and R would have prevented the torsional oscillations and the failure of the structure in the 42-mile wind that destroyed it. In fact they would have assured torsional stability at a wind of more than 100 miles an hour. If the girder depth had been twice as great, the numerical increases in K obtainable by adding the wind trusses would be quadrupled [6, 12].

Although the addition of wind trusses in two horizontal planes is highly effective against torsional oscillations, this method is far surpassed in economy and effectiveness by the simpler device of installing transverse diagonal stays (fig. 27). With diagonal wire-ropes only one-fifth of the lightest wind-bracing section assumed in the foregoing, the transverse diagonal stays would yield a 50-times greater augmentation of K, also a correspondingly greater augmentation of R [6, 12].

These simple and economical applications of stays can be effectively used to prevent aerodynamic oscillations in new bridges as well as to cure aerodynamic instability in existing bridges.

The Aerodynamic Solution

By increasing depth, rigidity, and bracing; by adding center stays, longitudinal diagonal stays, transverse diagonal stays, or other stays; and by introducing artificial damping devices, resistance to aerodynamic instability may be built up to any desired amount. These methods resist or check the effects but do not eliminate the cause.

The more scientific attack is the application of aerodynamic principles and methods to the selection or modification of the cross-section so as to minimize or eliminate any potential vulnerability.

The *slopes* of the lift and torque graphs (from simple wind-tunnel tests on small section models) are a measure of the potential instability. A positive slope identifies a *stable* section, with oscillations limited to low wind velocities (below the critical velocity) and usually negligible or damped. A negative slope identifies an *unstable* section, with an unlimited catastrophic range of oscillations *above* a critical wind velocity. The ideal lift or torque graph approximates a horizontal straight line; this identifies a seicton stable at all wind velocities and all angles of attack. The *curvature* of the lift graph or torque graph affects or determines the limiting amplitudes by determining the reduction of *mean* effective slope with increasing amplitude. The static wind-tunnel graphs for any section are thus a means of diagnosis, prediction, and prescription [12, 14, 15].

Fig. 28. Open Slots in Bridge Deck Yield Aerodynamically Stable Section. This feature Now Adopted in the Design or Reconstruction of All Large Suspension Bridges.
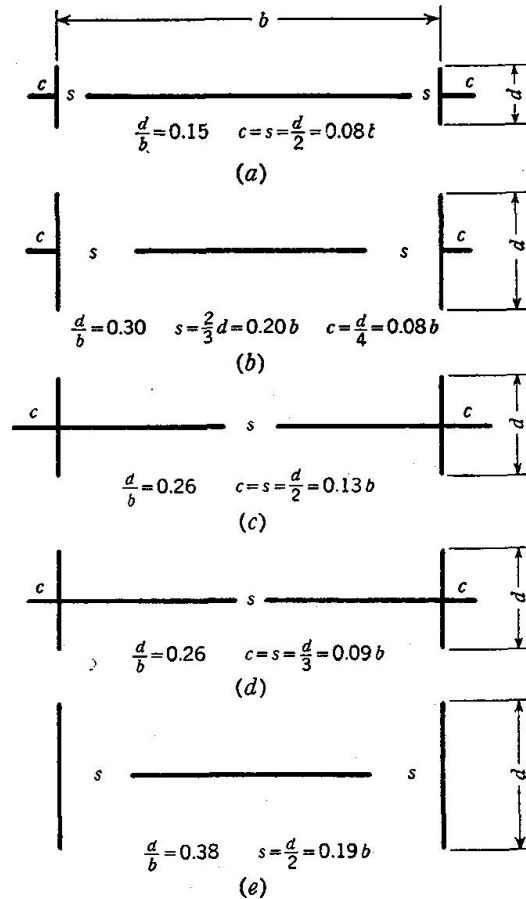

Fig. 29. Aerodynamically Stable Bridge Sections. Combinations of Slots and Fins Provide Complete Aerodynamic Stability.

By providing open slots at predetermined points of the roadway width (fig. 28), the aerodynamic forces causing amplification of oscillations can be eliminated or materially reduced. The most important horizontal area to leave open is between the edge of the roadway and the stiffening girder or truss chord. The opening of these lateral areas definitely reduces the net aerodynamic instability and may eliminate it.

That aerodynamic stability or instability of a section is a function of the form and proportions of the section and can be controlled by providing suitably located and proportioned openings in the horizontal width of the section, is now a demonstrated fact. Bridge cross-sections can be devised or modified to produce assured aerodynamic stability [6, 16].

In 1946/47 I undertook a systematic exploration of the aerodynamic pro-
perties of various forms and proportions of bridge cross-sections and of various
indicated modifications of such sections. To this end, I secured the generous
cooperation of Prof. F. J. MAHER, utilizing the wind tunnel facilities of the
Virginia Polytechnic Institute. With the help of a grant from the Research
Corporation, the test program was extended and amplified. The tests covered
a wide range of section-ratios and various modifications of the sections, includ-
ing open-grid roadway, lateral slots in roadway, center slot in roadway, and
outside fins. Such fins may take the form of cantilever brackets utilized for
sidewalks or other utilities. My original sugggestion of outside fins (in 1941) was
based on simple aerodynamic considerations. Subsequent research showed that
no bridge with outside brackets or cantilever sidewalks has ever been known to
show aerodynamic instability [16].

The 1947 wind-tunnel tests revealed that combinations of lateral slots and
outside fins in suitable proportions yield a complete cure or prevention of both
vertical and torsional instability. Such combinations of slots and fins had been
repeatedly suggested by me since 1941 in my published contributions.
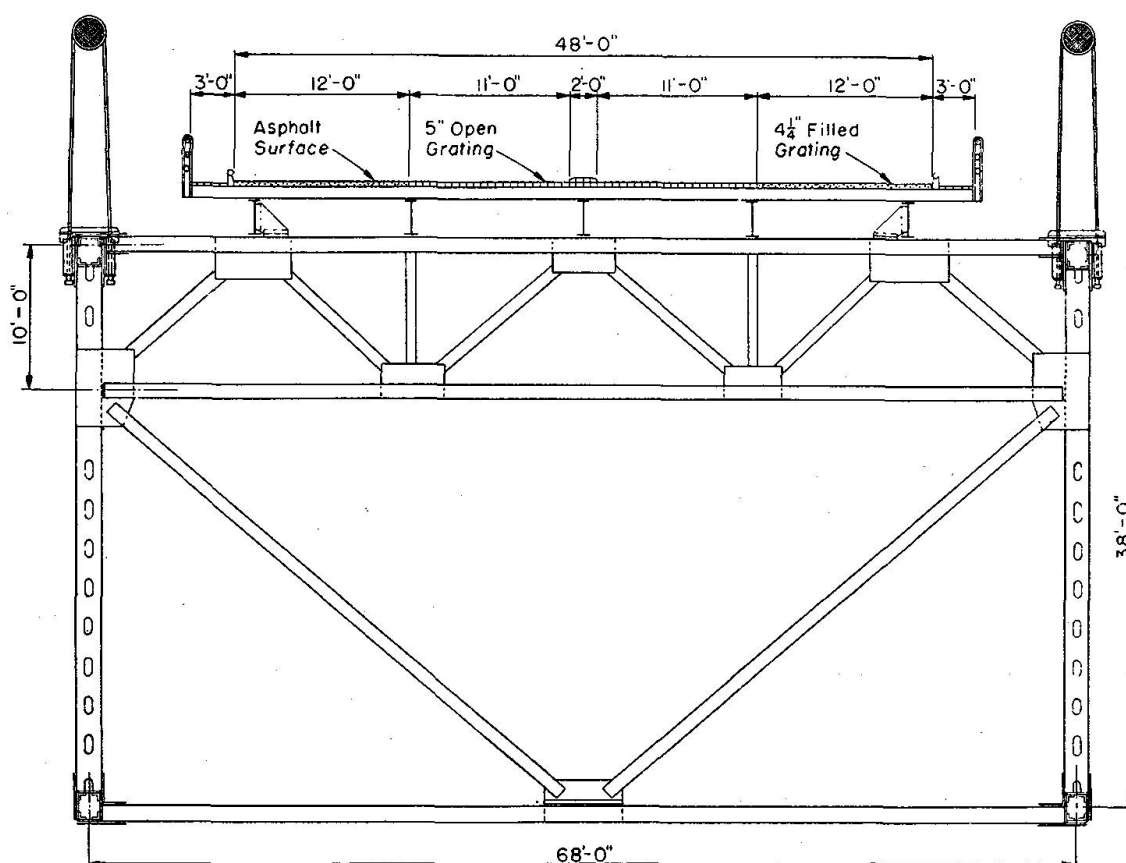

Fig. 30. Aerodynamically Stable Cross-Section Adopted for The Mackinac Straits Bridge,
Michigan, 1953. Lateral Openings, Central Openings, Open Trusses, Open Floorbeams,
and Top and Bottom Lateral Bracing Assure Aerodynamic Stability. Confirmed by Wind-
Tunnel Tests as the Most Stable Bridge Section Ever Designed. (Designed by the Author.)

Based on the foregoing wind-tunnel research, diagrams of some aerodynamically stable bridge sections (limited here to girder H-sections) are recorded in fig. 29. These modified sections offer complete aerodynamic stability, vertical, torsional, and coupled, for all angles of incidence and at all wind velocities [16].

An application of the foregoing principles to a practical bridge cross-section is shown in fig. 30. This is the adopted cross-section for the Mackinac Straits Bridge of 3800 feet span. The design features of wide lateral openings (between roadway and truss chords) and a wide central opening (two inner roadway lanes of open-grid construction), in combination with deep open-web stiffening trusses and open-web floorbeams, yield a most highly favorable section. Windtunnel tests confirm the high aerodynamic stability, and indicate that this is the most stable section, aerodynamically, ever designed. In addition, a double system of lateral bracing (top and bottom) provides very high torsional rigidity, so that the bridge has its aerodynamic stability doubly assured [18].

By the various means of stiffening and bracing, resistance to the effects of aerodynamic instability may be built up to any desired degree. By scientific design of the cross-section, applying aerodynamic findings and concepts, the cause of instability can be eliminated. The one line of attack places the emphasis on providing increased resistance to a dangerous inherent characteristic; the other aims to avoid or eliminate the dangerous characteristic.

It is more scientific to eliminate the cause than to build up the structure to resist the effect. The aerodynamic or fluid mechanics phase of the problem was the real challenge to engineers and scientists. In response to this challenge, we now have the new science of Bridge Aerodynamics [19].

References

1. D. B. STEINMAN: "Bridges and Aerodynamics", *Proceedings*, Amer. Toll Bridge Assoc., March, 1941, pp. 1—9.
2. — "Aerodynamics of Suspension Bridges", *Proceedings*, Thirty-Second Annual Roads School, Purdue University, January, 1946, pp. 26—38.
3. — "Design of Bridges Against Wind. 1. General Considerations — Aerostatic Stability", *Civil Engineering*, October, 1945, pp.469—472.
4. — "Design of Bridges Against Wind. II. Aerodynamic Instability — Historical Background", *Civil Engineering*, November, 1945, pp. 501—504.
5. — "Design of Bridges Against Wind. III. Elementary Explanation of Aerodynamic Instability", *Civil Engineering*, December, 1945, pp. 558—560.
6. — "Design of Bridges Against Wind. IV. Aerodynamic Instability — Prevention and Cure". — *Civil Engineering*, January, 1946, pp. 20—23.
7. — "Design of Bridges Against Wind. V. Criteria for Assuring Aerodynamic Stability", *Civil Engineering*, February, 1946, pp. 66—68.
8. "The Tacoma Bridge Report", *Engineering News-Record*, August 14, 1941, pp. 59, 61.
9. — "Wind Tunnel Tests Reveal Serious Inadequacy of Present Bridge Specifications", *Civil Engineering*, October, 1947, pp. 35—38.

10. D. B. Steinman: "Problems of Aerodynamic and Hydrodynamic Stability", *Proceedings*, Third Hydraulics Conference, Bulletin No. 31, State University of Iowa Studies in Engineering, Iowa City, Iowa, 1947, pp. 136—164.

11. — "Pipeline Bridge Stabilized with Diagonal Rope Stays", *Civil Engineering*, March, 1952, pp. 25—27.

12. — "Rigidity and Aerodynamic Stability of Suspension Bridges", *Transactions*, Am. Soc. C. E., Vol. 110, 1945, pp. 439—580.

13. — "Aerodynamic Theory of Bridge Oscillations", *Transactions*, Am. Soc. C. E., Vol. 115, 1950, pp. 1180—1260.

14. — "Simple Model Tests Predict Aerodynamic Characteristics of Bridges. Part I. Response Curves Computed from Pressure Distribution Graphs", *Civil Engineering*, January, 1947, pp. 20—23.

15. — "Simple Model Tests Predict Aerodynamic Characteristics of Bridges. Part II. Response Curves Computed from Static Lift and Torque Graphs", *Civil Engineering*, February, 1947, pp. 77—79.

16. — "Wind Tunnel Tests Yield Aerodynamically Stable Bridge Sections — Tests Provide Data on Effects of Slots and Fins on Stability", *Civil Engineering*, December, 1947, pp. 40—43.

17. — "The Messina Straits Bridge", *Columbia Engineering Quarterly*, Columbia University, January, 1951, pp. 8—30.

18. — "Engineering Report on Mackinac Straits Bridge", *Report* to the Mackinac Bridge Authority, State of Michigan, February 20, 1953, pp. 1—18.

19. F. J. Maher: "Tests Confirm Steinman Theory of Bridge Oscillations", *Civil Engineering*, August, 1953, pp. 66—67.

Summary

Some bridge failures, such as the catastrophe of the Tacoma Bridge (November 1940) has required the creation of a new science, *Bridge Aerodynamics*. With regard to the aerodynamic action of wind, its vertical component is more dangerous than the horizontal component.

The stability or instability of a section depends on the „velocity ratio" V/Nb, where V signifies the wind velocity, N the natural frequency of the oscillating structure and b the width of the section.

In order to amplify the test procedure and perfect the mathematical analysis, the writer used models with curved cross-sections.

Methods of augmenting rigidity and structural damping are provided by cable stays, center stays, intermediate diagonal stays and transverse diagonal stays (e. g. Deer Isle Bridge 1943, Mackinac Straits Bridge 1953).

Résumé

Divers accidents survenus sur des ponts aux Etats-Unis et tout particulièrement la catastrophe du pont de Tacoma en novembre 1940 ont conduit à traiter l'influence des efforts dûs au vent, non seulement sous la forme statique, mais également sous la forme aérodynamique.

Les mouvements verticaux provoqués par le vent dans l'ouvrage sont considérés comme particulièrement dangereux. Pour maintenir dans les limites admissibles les mouvements verticaux et les mouvements de torsion correspondant à un vent horizontal déterminé, il faut faire intervenir non seulement la largeur, mais aussi la forme de la section du tablier, ainsi que la flèche du câble par rapport à la portée.

Pour compléter les théories déjà connues en matière d'oscillations, on a procédé à des essais en soufflerie sur des sections incurvées.

Pour obtenir la rigidité nécessaire dans les ponts suspendus, il est recommandé de prévoir des câbles en diagonale (entre le câble porteur et le tablier), ainsi que des contreventements verticaux au-dessous du tablier (pont Deer Isle 1943, pont Mackinac Straits 1953).

Zusammenfassung

Verschiedene Brückeneinstürze in den USA, vor allem die Katastrophe der Tacoma-Brücke (November 1940) führten dazu, die Wirkung der Windkräfte nicht nur als statisches, sondern als *aerodynamisches* Problem zu behandeln.

Als besonders gefährlich werden die durch den Wind verursachten Vertikalbewegungen des Bauwerks angesehen. Damit die Vertikal- und Torsions-Bewegungen für eine bestimmte horizontale Windkraft in erträglichen Grenzen bleiben, kommt es neben der Breite auch auf die Form des Fahrbahnquerschnittes und auf die Pfeilhöhe des Kabels im Verhältnis zur Spannweite an.

Zur Ergänzung der aufgestellten Schwingungstheorien wurden auch Versuche mit gekrümmten Querschnitten im Windkanal unternommen.

Zur Erreichung der notwendigen Steifigkeit bei Hängebrücken werden Diagonal-Kabel (zwischen Tragkabel und Fahrbahn) und vertikale Windverbände unter der Fahrbahn empfohlen (Deer Isle Bridge 1943, Mackinac Straits Bridge 1953).

Leere Seite

Blank page

Page vide